—Review—

ナノマテリアルの慢性影響研究の重要性

広瀬明彦,*,[a] 高木篤也,[a] 西村哲治,[a] 津田洋幸,[b] 坂本義光,[c]
小縣昭夫,[c] 中江　大,[c] 樋野興夫,[d] 菅野　純[a]

Importance of Researches on Chronic Effects by Manufactured Nanomaterials

Akihiko HIROSE,*,[a] Atsuya TAKAGI,[a] Tetsuji NISHIMURA,[a]
Hiroyuki TSUDA,[b] Yoshimitsu SAKAMOTO,[c] Akio OGATA,[c]
Dai NAKAE,[c] Okio HINO,[d] and Jun KANNO[a]

[a]Division of Risk Assessment, National Institute of Health Sciences, Kamiyoga 1-18-1, Setagaya-ku, Tokyo 158-8501, Japan, [b]Nagoya City of University, 1 Kawasumi Mizuho-cho, Mizuho-ku, Nagoya 467-8601, Japan, [c]Tokyo Metropolitan Institute of Public Health, 3-24-1 Hyakunin-cho, Shinjyuku-ku, Tokyo 169-0073, Japan, and [d]Juntendo University School of Medicine, 2-1-1 Hongo, Bunkyo-ku, Tokyo 113-8421, Japan

(Received September 3, 2010)

Manufactured nanomaterials are the most important substances for the nanotechnology. The nanomaterials possess different physico-chemical properties from bulk materials. The new properties may lead to biologically beneficial effects and/or adverse effects. However, there are no standardized evaluation methods at present. Some domestic research projects and international OECD programs are ongoing, in order to share the health impact information of nanomaterails or to standardize the evaluation methods. From 2005, our institutes have been conducting the research on the establishment of health risk assessment methodology of manufactured nanomaterials. In the course of the research project, we revealed that the nanomaterials were competent to cause chronic effects, by analyzing the intraperitoneal administration studies and carcinogenic promotion studies. These studies suggested that even aggregated nanomaterials were crumbled into nano-sized particles inside the body during the long-term, and the particles were transferred to other organs. Also investigations of the toxicokinetic properties of nanomaterials after exposure are important to predict the chronically targeted tissues. The long lasting particles/fibers in the particular tissues may cause chronic adverse effects. Therefore, focusing on the toxicological characterization of chronic effects was considered to be most appropriate approach for establishing the risk assessment methods of nanomaterials.

Key words——chronic toxicity; multi-wall carbon nanotube (MWCNT); fullerene

1. はじめに

近年，ナノテクノロジーの中心的な役割を担う物質としての産業用ナノマテリアルは，急速にその種類や生産量が増加しつつあるところであるが，新たに期待されているナノマテリアルの物理化学特性については，有効的な生理活性等に使用され得る特性を持つ反面，ヒト健康影響に対する懸念についても検証されるべきであると考えられている．つまり，ナノマテリアルを用いた技術や製品を社会的に受容するためには，安全性の検証を行うことが不可欠であると思われる．しかし，従来の一般的な化学物質とは異なる物理化学的特性は，その毒性評価においても従来とは異なる考え方を取り入れることも必要とされている．それゆえ，ナノマテリアルの特性を考慮した有害性評価手法の開発が急務となっている．また，国際的な枠組みにおいても，ナノマテリアルの安全性確認は，重要な問題として認識されており，OECD や ISO 等を中心として評価手法の国際的標準化に向けた取り組みが進行しているところでもある．本稿では，ナノマテリアルの安全性評価

[a]国立医薬品食品衛生研究所（〒158-8501 東京都世田谷区上用賀 1-18-1），[b]名古屋市立大学（〒467-8601 名古屋市瑞穂区瑞穂町字川澄 1），[c]東京都健康安全研究センター（〒169-0073 東京都新宿区百人町 3-24-1），[d]順天堂大学医学部（〒113-8421 東京都文京区本郷 2-1-1）
*e-mail: hirose@nihs.go.jp

本総説は，日本薬学会第 130 年会シンポジウム S18 で発表したものを中心に記述したものである．

の確立に向けたこれらの取り組みに貢献してきたわれわれの研究成果の一部と，それらの研究結果から帰納的に導き出された慢性影響評価研究の重要性について論ずる．

2. ナノマテリアルのリスク評価法の確立における課題

一般的に，化学物質の健康影響評価（リスクアセスメント）の基本的なフレームは，有害性評価と曝露評価，及び各々の評価内容を比較・統合化する過程のリスク判定のステップから成り立っている．この基本的なフレーム自体は，ナノマテリアルの健康影響評価に適用できるものであると考えられる．[1-5] しかし，ナノマテリアルに特徴的な新たな物理化学的性質，特にサイズが生体内高分子と近いことや，高い表面活性のために凝集し易い性質を考慮すると，よりサイズの大きい通常のバルク化合物や完全に溶解した単一分子化合物とは，生体内挙動が異なることが予想され，同じ化学組成の化合物であってもその毒性発現部位や発現様式は異なることが予想される．つまり，体内動態［吸収 absorption，分布 distribution，代謝 metabolism，排泄 excretion（ADME）］情報は，一般の化学物質より重要な意味を持つと考えられる．

そこで，生体内での挙動を把握するためには，生体試料中で検出，同定・定量できる方法を確立しなくてはならない．一般にナノマテリアルの開発段階において，その性質を把握するための物理化学的測定法も同時に開発されているはずであるが，それらの手法は生体試料中に存在するナノマテリアルにそのまま適用できないことも多い．さらに，機器分析法による生体試料中での検出や定量が可能になったとしても，生体内で実際にナノの状態で存在しているのか，あるいは再凝集などはしていないかなど，標的組織における最終的な生体内反応に影響を及ぼすと考えられる実際のナノマテリアルの存在状態を把握するためには，最終的には，組織標本の電子顕微鏡などによる確認が必要となる．

一方，体内動態に影響を与える因子として，投与法を検討する必要もある．単独では凝集し易いナノマテリアルをそのまま曝露するということは，物理的に巨大となった粒子は体への吸収性が低く，ナノマテリアル自体の体内動態や懸念される有害性を検出することが困難になると考えられるためである．そのために曝露実験時におけるナノマテリアルの分散手法の開発が必要となる．職業曝露などの比較的大量のナノマテリアル曝露の安全性を評価するという観点からは，凝集したままの曝露にも意義があるかもしれないが，製品中への混入や環境中への排出を経由した，分散された曝露も想定されることは考慮すべきであると考えられる．

Figure 1 は，凝集したナノマテリアルが，生体に取り込まれた場合に想定される体内動態を模式図化したものである．ナノマテリアルの使用用途にも依存するが，製品中のナノマテリアルはポリマー等の他の高分子化合物等と混合された状態，あるいはナノマテリアルだけが単独で製品から解離していく状態を考慮しても，この凝集性のために，大きな粒子として曝露する可能性が高いものと想定される．急性的には，このサイズの大きくなった物質は生体に取り込まれることはほとんどなく，局所的な刺激を起こすような変化を除いては，生体内で有害性が惹起される可能性は低いものと考えられる．しかし，仮に凝集したナノマテリアルが長期間に渡って，吸収部位である肺胞や消化管，損傷皮膚などの局所に滞留したり，慢性的に曝露したりするケースを想定すると，時間経過とともに小さくなった凝集体の粒子を除去するために，マクロファージなどの食細胞による取り込みや，表面活性の高いナノマテリアル分子と生体成分との結合作用による侵食作用により，生体に少しずつ取り込まれることが想定される．もしも生体内に取り込まれたナノマテリアルと生体内成分との結合性が高い場合には，容易に生体外に排出されることはなく，特定の組織等へ蓄積し易くなり，慢性影響の可能性を検討する必要が出てくると想定できる．

3. 国立医薬品食品衛生研究所における取り組みの成果の概要

以上のナノマテリアル固有の検討課題を考慮して，われわれは 2005 年より厚生労働科学研究の化学物質リスク研究事業の枠組みの中で，ナノマテリアルの健康影響評価手法の開発に係わる研究を推し進めてきたところである．われわれは，これらの検討課題を解決するために，Fig. 2 に示すように 4 つの項目を中心に研究を行ってきた．これらの項目の中で，*in vivo* 研究については，比較的研究初期の段階から中心的に取り組んできた．その中で，繊維

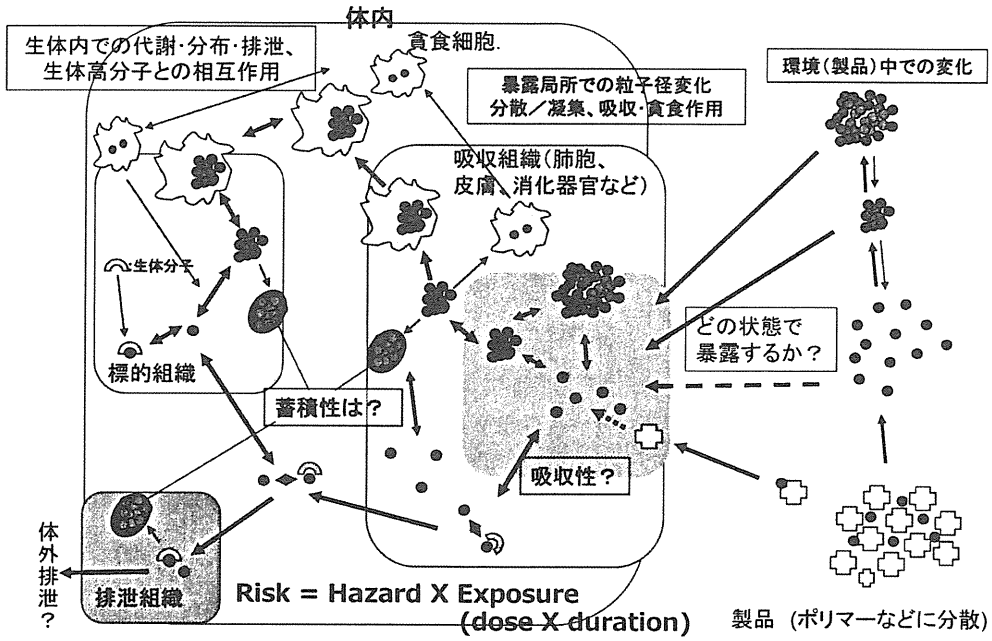

Fig. 1. The Estimated ADME Schema of Nanomaterials

*in vivo*試験法研究

MWCNTのP53ヘテロ欠失マウスへのi.p.投与による中皮腫誘発性を確認
バイオマーカとしてマウスのメソセリン抗体の作成
一方、C60の腹腔内投与による慢性的影響として腎臓への影響を示唆
TiO_2と C60の気管内投与による発がんプロモーション作用の示唆

吸入試験法研究

MWCNTのミスト暴露システムを開発
気管内投与時の分散性依存の発現様式差異を確認
リポソーム分散C60による気管内投与法を開発。

暴露測定法／動態解析研究

生体試料でのC60の定量的検出法との確立
静注後のC60の組織からの経時的消失検討
気管内投与後のMWCNTの肺及び肝臓での検出

*in vitro*試験法研究

細胞培養系でのリポソーム等を用いた分散法の確立
→C60やTiO_2の遺伝毒性、細胞透過性、
神経系の細胞機能への影響、などへの適用

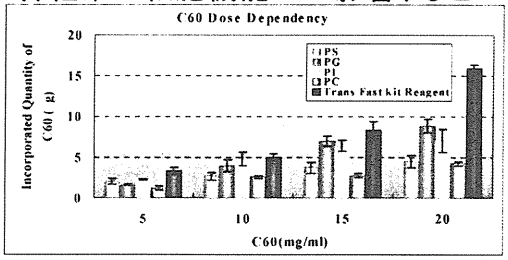

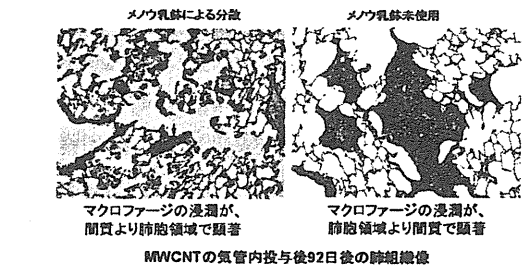

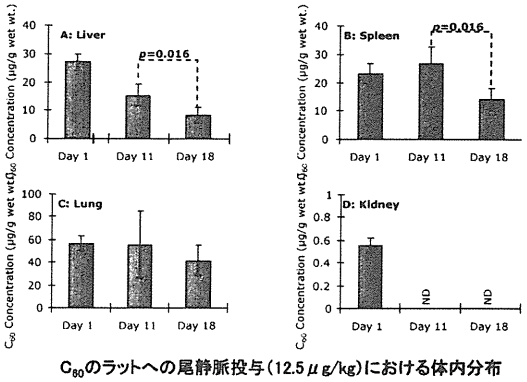

C_{60}のラットへの尾静脈投与（12.5 μg/kg）における体内分布
反復(4回)投与後の体内分布の経時変化

Fig. 2. The Overall Results of NIHS Projects for Nanomaterial Safety

長の長いタイプの多層型カーボンナノチューブ（MWCNT）が，中皮腫を誘発する可能性を持つことを確認した.[6] 上記の体内動態の重要性を考慮した概念からは，吸収性や体内分布について検証したのちに，慢性影響の可能性を検討することが論理的であるが，研究開始当時から，大量生産可能であった，酸化チタン（TiO_2）やフラーレン（C60），MWCNTについては，*in vivo* の慢性影響を先行して検討しておくべきであると判断した．特にその形状がアスベストに似ていたMWCNTについては，吸入曝露による有害影響が懸念されたが，MWCNTについての吸入曝露法が確立していない段階では，アスベストでも検証に使用されていた腹腔内投与による中皮腫誘発試験を行うこととした．

われわれの最初の実験は，アスベストで中皮腫の誘発時期が早くなることが知られているp53ヘテロノックアウトマウスへの腹腔内へ3 mg/mouseという高用量を投与することによって確認されたものであり，動物種の特異性や投与量の多さについて異論も指摘された．しかしその後の研究で，野生型の動物種であるF344ラットに対しても，同じMWCNTが中皮腫の誘発作用を持つことが確認された[7]ほか，投与量を1000分の1にまで少なくした実験においても中皮腫の起きることが示されている（投稿中）．

酸化チタンについては，雌ラットへの吸入曝露により発がん性のあることが示されているが，ナノサイズ化による発がん性の検証のために，気管内投与による肺がんのプロモーション作用の検討を行った．その結果，酸化チタンは，肺腺腫や乳腺腫に対してプロモーション作用を示し，その作用は，マクロファージから放出される炎症性因子であるMIP1αを介したものであることが示唆された.[8] 現在C60やMWCNTを用いたプロモーション作用の検討が進行中である．

一方，曝露手法の開発においては，ミスト法や粉体法によるMWCNTの吸入曝露システムの開発研究を進めているが，より簡易な手法として気管内投与のための適切な分散法の検討を行った．その結果，分散法の違いが肺の有害性発現様式に違いを引き起こすことを確認した.[9]

体内動態解析のために，生体試料中のC60やTiO_2の分析手法の開発や改良を行い，経口投与や気管内投与による体内吸収性について検討を行っている．現在のところ投与部位である消化管や肺以外で有意な検出量を確認できておらず，感度の向上に向けた研究を進めている．しかし，体内への吸収を前提にした解析として，C60の静脈内投与による解析を行ったところ，肝臓や脾臓，肺などへの分布を確認したが，腎臓への分布は極めて低いことが示された（投稿中）．その他，遺伝毒性や標的臓器などの毒性をスクリーニングするための *in vitro* 試験における培地等への分散法も検討対象としており，リポソームを用いたC60の分散法を確立した．

4. 慢性影響研究の重要性

ナノマテリアルの生体影響に関する情報はここ数年の活発な研究状況を反映して多くなりつつあるが，慢性影響に関する報告は依然その数が少ない状況である．一般の化学物質の有害性評価の常套手段として，変異原性試験や短期試験から情報を収集していくことは，必要なステップであり，OECDにおけるナノマテリアル作業グループの活動におけるスポンサーシッププログラムにおいても，加盟各国からの毒性試験情報として，短期試験を中心に収集されてきている．われわれの研究グループにおいても，これらの枠組みに対して，短期的な試験情報を中心に提供し始めている段階である．しかしMWCNTに関しては，研究初期から，短期毒性より長期毒性の方が懸念の強いことが，物性等の情報から推測されたところでもあり，その推定に基づいて，腹腔内投与の研究を最初にスタートさせた．腹腔内投与は，リスク評価の観点からは，曝露経路（吸入曝露）に伴う定量的な評価に問題のあるところであるが，最近の注目すべき研究として，分散剤で分散させたMWCNT（最高80 μgまで）をマウスに吸引させた研究や，MWCNT: 30 mg/m^{3}をマウスに単回吸入曝露した研究において，曝露後7–8週間目にMWCNTが胸膜に到達していたことが報告されている.[10,11] これらの研究結果は高用量の曝露による短期間の結果ではあるが，呼吸器を経由した曝露においてもMWCNTは胸膜（中皮）まで到達することを示唆しており，われわれの腹腔内投与による結果と合わせると，リスク評価の上でも重要な知見であると考えられる．

これらの腹腔内投与による中皮腫誘発能は，繊維状粒子による催腫瘍性のみを検出する系であり，短

いタイプやその他様々な形状のMWCNTにおける慢性毒性は別途検証する必要性がある．実際，われわれの行った腹腔内投与試験では，小さいサイズのナノチューブ繊維を含んだ細胞が腹膜の病変部のみならず，肝類洞内，又は肝葉間や腸間膜リンパ節の中にも認められ，体内に再分布することが示唆された（Fig. 3）.[6] さらに，SWCNTをマウスへ咽頭吸引させた実験では，一過性の急性症状の後に，炎症性細胞浸潤を伴わない間質の繊維化が認められている.[12] また，ApoEノックアウトマウスを用いた実験では，タンパクカルボニル化活性の変化を伴うミトコンドリアDNA障害と，アテローム性動脈硬化症の進行を増強することが示された.[13] MWCNTに関しても，マウスにMWCNT（200–400 μg）を気管内滴下した実験では，一過性の肺の炎症反応に加え，投与量に依存した血小板の活性化と凝固作用の活性化の促進が示唆されている.[14] また，MWCNTやSWCNTの気管内投与や経鼻投与により，アレルギー反応の増強反応が報告されている.[15-17] これらの結果が，カーボンナノチューブが直接体内循環に侵入した結果であるか，免疫細胞との接触を介した反応であるかを区別することは難しいが，曝露局所に留まらない全身作用の可能性を示している．われわれの酸化チタンの気管内投与による発がんプロモーション作用が，炎症因子により介在されたことは，これらの知見と同様の作用様式を示すものととらえることもできる．

以上の知見は，短期の試験だけでは検証することは困難であり，ナノマテリアルの有害性を確認するためには，長期の体内動態予測や慢性影響に関する研究が，重要なステップであることを示している．Figure 4にスクリーニング試験や確定試験を開発するための手順についてまとめた．通常の化学物質については，その長い歴史の中で明らかとなった有害性に対して，それぞれの毒性発現様式に応じてスクリーニング試験が開発され，現在まで運用されてきている．特に変異原性試験は発がん性を予測する試験としての重要な役割を担っている．しかし，現時点ではナノマテリアルによる有害性影響が，これまでの研究経験の中で明らかとなった影響だけに留まるのかについては，まだ誰も判定できない状況である．これまでの一般化学物質に対応する有害性とスクリーニング試験を活用して進めていくと同時に，未知の影響を見極める最初のステップとして，少な

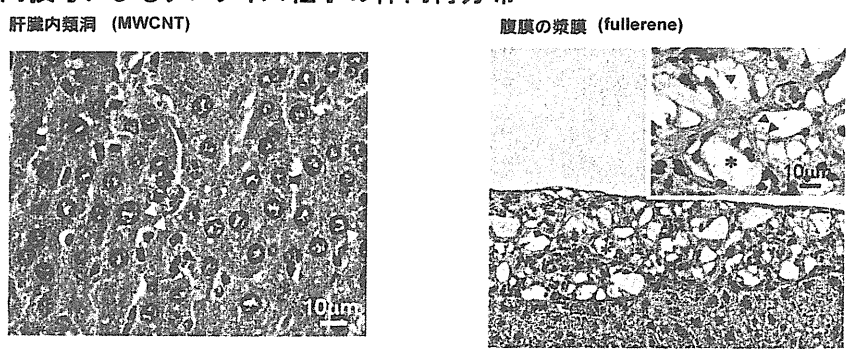

A. Takagi et al., J. Toxicol. Scie., **33**,105-116. (2008)

SWCNTやMWCNTによる全身性影響の示唆

•アテローム性動脈硬化症の進行の増強の可能性（ApoE$^{-/-}$マウス）
Z. Li *et al.*, *Environmental health perspectives*. **115**, 377-382 (2007)

•血小板の活性化と凝固作用の活性化（MWCNT気管内滴下）
A. Nemmar *et al.*, *J. Thrombosis, Haemostasis* **5:** 1217-1226 (2007)

•アレルギー反応の増強（MWCNT・SWCNT、気管内・経鼻投与）
E.J. Park *et al.*, *Toxicology*. **259**, 113-21 (2009)
U.C. Nygaard *et al.*, *Toxicol Sci*. **109**, 113-23 (2009)
K. Inoue *et al.*, *Toxicol Appl Pharmacol*. **237**, 306-16 (2009)

Fig. 3. The Suggestive Evidences for Systemic Toxicites by Nanomaterials

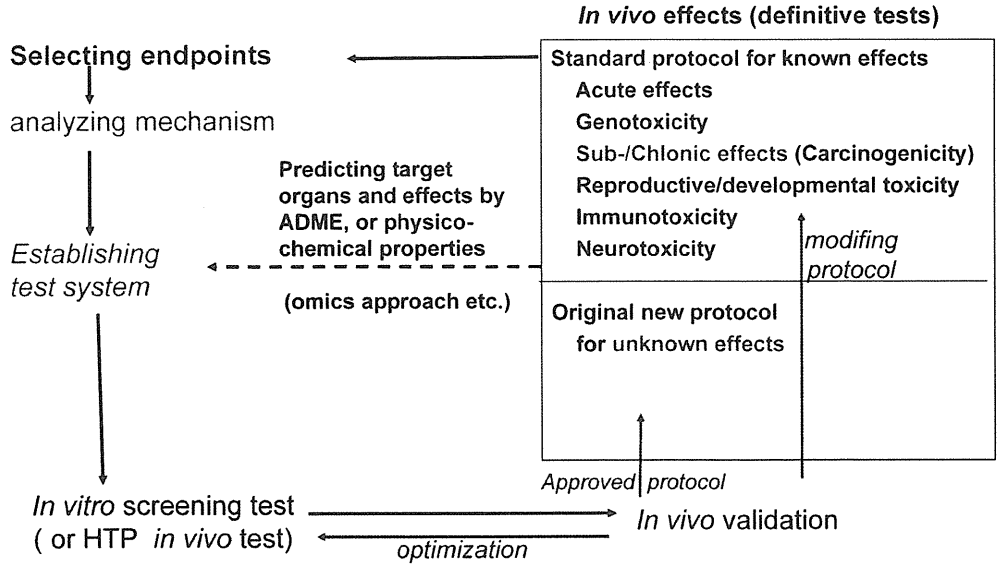

Fig. 4. The Schematic Development of Screening Tests and Definitive Tests

くとも代表的なナノマテリアルによる *in vivo* の慢性影響研究や，その影響を推定するためのナノマテリアルと生体成分との分子レベルでの相互作用や体内残留性様式の解析を進めていくべきであると考えられる．

謝辞　本稿で解説した研究成果の一部は，厚生労働科学研究費補助金（化学物質リスク研究事業）H17-化学-012，H18-化学--一般-007 及び H21-化学--一般-008 の助成によって行われたものです．

REFERENCES

1) Scientific Committee on Emerging and Newly Identified Health Risks, SCENIHR: ⟨http://ec.europa.eu/health/ph_risk/committees/04_scenihr/docs/scenihr_o_003b.pdf⟩, European Commission Web, cited 14 November, 2010.
2) Scientific Committee on Emerging and Newly Identified Health Risks, SCENIHR: ⟨http://ec.europa.eu/health/ph_risk/committees/04_scenihr/docs/scenihr_o_010.pdf⟩, European Commission Web, cited 14 November, 2010.
3) Food Safety Authority of Ireland, FSA, "The Relevance for Food Safety of Applications of Nanotechnology in Food and Feed Industries," Dublin, 2008.
4) UK Committees on Toxicity, Mutagenicity and Carcinogenicity of Chemicals in Food, Consumer Products and the Environment (COT, COM, COC): ⟨http://cot.food.gov.uk/pdfs/cotstatements2005nanomats.pdf⟩, COT Web, cited 14 November, 2010.
5) The Committee on Toxicity of Chemicals in Food, Consumer Products and the Environment: ⟨http://www.food.gov.uk/multimedia/pdfs/cotstatementnanomats200701.pdf⟩, cited 14 November, 2010.
6) Takagi A., Hirose A., Nishimura T., Fukumori N., Ogata A., Ohashi N., Kitajima S., Kanno J., *J. Toxicol. Sci.*, **33**, 105–116 (2008).
7) Sakamoto Y., Nakae D., Fukumori N., Tayama K., Maekawa A., Imai K., Hirose A., Nishimura T., Ohashi N., Ogata A., *J. Toxicol. Sci.*, **34**, 65–76 (2009).
8) Xu J., Futakuchi M., Iigo M., Fukamachi K., Alexander D. B., Shimizu H., Sakai Y., Tamano S., Furukawa F., Uchino T., Tokunaga H., Nishimura T., Hirose A., Kanno J., Tsuda H., *Carcinogenesis*, **31**, 927–935 (2010).
9) Wako K., Kotani Y., Hirose A., Doi T., Hamada S., *J. Toxicol. Sci.*, **35**, 437–446 (2010).
10) Nurkiewicz T. R., Porter D. W., Hubbs A. F., Stone S., Chen B. T., Frazer D. G., Boegehold M. A., Castranova V., *Toxicol. Sci.*, **110**, 191–203 (2009).
11) Ryman-Rasmussen J. P., Cesta M. F., Brody

A. R., Shipley-Phillips J. K., Everitt J. I., Tewksbury E. W., Moss O.R., Wrong B. A., Dodd D. F., Andersen M. E., Bonner J. C., *Nat. Nanotechnol.*, **4**, 747–751 (2009).

12) Shvedova A. A., Kishin E. R., Mercer R., Murray A. R., Johnson V. J., Potapovich A. I., Tyurina Y. Y., Gorelik O., Arepalli S., Schwegler-Berry D., Hubbs A. F., Antonini J., Evans D. E., Ku B. K., Ramsey D., Maynard A., Kagan V. E., Castranova V., Baron P., *Am. J. Physiol. Lung cell. mol. physiol.*, **289**, L698–L708 (2005).

13) Li Z., Hulderman T., Salmen R., Chapman R., Leonars S. S., Young S. H., Shvedova A., Luster M. I., Simeonove P. P., *Environ. Health Perspect.*, **115**, 377–382 (2007).

14) Nemmar A., Hoet P. H., Vandervoort P., Dinsdale D., Nemery B., Hoylaerts M. F., *J. Thromb. Haemost.*, **5**, 1217–1226 (2007).

15) Park E. J., Cho W. S., Jeong J., Yi J., Choi K., Park K., *Toxicology*, **259**, 113–121 (2009).

16) Nygaard U. C., Hansen J. S., Samuelsen M., Alberg T., Marioara C. D., Løvik M., *Toxicol. Sci.*, **109**, 113–123 (2009).

17) Inoue K., Koike E., Yanagisawa R., Hirano S., Nishikwa M., Takano H., *Toxicol. Appl. Pharmacol.*, **237**, 306–316 (2009).

Genes and Environment, Vol. 33, No. 1 pp. 27-31 (2011)

Short communication

Fullerene (C_{60}) Is Negative in the *In Vivo Pig-A* Gene Mutation Assay

Katsuyoshi Horibata[1,5], Akiko Ukai[1], Naoki Koyama[1], Atsuya Takagi[2], Jun Kanno[2], Takafumi Kimoto[3], Daishiro Miura[3], Akihiko Hirose[4] and Masamitsu Honma[1]

[1]Division of Genetics and Mutagenesis, National Institute of Health Sciences, Tokyo, Japan
[2]Division of Toxicology, National Institute of Health Sciences, Tokyo, Japan
[3]TEIJIN Pharma Limited, Tokyo, Japan
[4]Division of Risk Assessment, National Institute of Health Sciences, Tokyo, Japan

(Received December 24, 2010; Revised January 20, 2011; accepted January 21, 2011)

Carbon nanoparticles, such as carbon nanotubes and fullerene (C_{60}), are potential candidates as leading substances in nanotechnological fields, but little is known about their safety. Here we examined *in vivo* genotoxicity of C_{60}, by performing the *Pig-A* gene mutation assay in the peripheral blood of male C57BL/6Cr mice. Mice were given single intraperitoneal injection of 3 mg of C_{60} particles in 0.5 mL suspension containing 0.1%-Tween80-saline. As a positive control for the *Pig-A* gene mutation assay, mice were given a single oral administration of *N*-nitroso-*N*-ethylurea. At 2 and 8 weeks after treatments, we analyzed CD24-negative and -positive red blood cells in peripheral blood and calculated *Pig-A* mutant frequencies. As a result, we detected no significant differences in the mutant frequencies between C_{60} treated and non-treated mice, indicating that C_{60} is negative for genotoxicity *in vivo* in the limited target tissues assessed in this study. For the full assessment, we need comprehensive whole body survey on the genotoxicity of C_{60}.

Key words: carbon nanoparticle, *in vivo* genotoxicity, *Pig-A* gene mutation assay, fullerene

Introduction

Manufactured nanomaterials are important substances in nanotechnology, and the potential human and environmental risks need to be investigated for risk assessment and management.

There are several reports on the toxicities induced by carbon nanoparticles, such as single-wall carbon nanotubes (SWCNTs), multi-wall carbon nanotubes (MWCNTs) and fullerene (C_{60}). Intraperitoneal application of MWCNTs induced mesothelioma in $p53^{+/-}$ mouse (1) and intrascrotal administration of MWCNTs induced mesothelioma in wild-type rats (2). Reports on the *in vivo* genotoxicity of C_{60}, however, are conflicting. It was reported that intratracheal instillation of C_{60} increased both mutation frequency detected by *gpt*-assay and DNA damage detected by comet assay in lung (3). Nevertheless another group showed that treatment with C_{60} by gavage has no genotoxical effect in ICR mice, using *in vivo* micronucleus test in bone marrow cells (4). These discrepancies could have been caused by differences in administration route, test method, or target organ.

Here we examined the *in vivo* genotoxicity of C_{60} using a different test system—the recently established *Pig-A* gene mutation assay (5,6). The *Pig-A* assay, a powerful tool for the evaluation of *in vivo* genotoxicity, is based on flow cytometric enumeration of glycosylphosphatidylinositol (GPI) anchor-deficient erythrocytes and has been shown to be applicable across species from rodent to monkey (5–8). With this method, we need no transgenic animals to test *in vivo* genotoxicity, but need only 1–2 μL peripheral blood (5,6). Additionally, long-term, accumulated *in vivo* genotoxic effects could be evaluated (9).

Materials and Methods

Test chemicals: Fullerene (C_{60}, Nanom purple SUH; purity >99.9%, Frontier Carbon Corporation, Tokyo, Japan) was obtained and prepared as previously described with some modifications (1). Briefly, C_{60} was suspended to physiological saline (Ohtsuka Pharmaceutical Co., Tokyo, Japan) and autoclaved. After addition of Tween 80 (Polysorbate 80 (HX), NOF Corporation, Tokyo, Japan) at a final concentration of 0.1%, solutions were subjected to sonication by ultrasonic homogenizer (VP30s, TAITEC Co. Japan). C_{60} was prepared at a final concentration of 6 mg/mL. *N*-nitroso-*N*-ethylurea (ENU, Sigma) was dissolved in PBS (pH

[5]Correspondence to: Katsuyoshi Horibata, Division of Genetics and Mutagenesis, National Institute of Health Sciences, 1-18-1 Kamiyoga, Setagaya-ku, Tokyo 158-8501, Japan. Tel: +81-3-3700-1141, Fax: +81-3-3700-2348, E-mail: horibata@nihs.go.jp

6.0) at 10 mg/mL as previously described (5).

Animal treatment: Mice were treated as described previously (1). In brief, 6 male wild-type C57BL/6Cr mice (SLC, Shizuoka, Japan) at the age of 9–11 weeks were given single i.p. injection of 3 mg/head suspension (0.5 mL) of C_{60}. Vehicle solution (0.5 mL) was given to 6 mice as negative controls. As a positive control of this study, 5 mice were given single oral administration of ENU (40 mg/kg). Peripheral bloods were withdrawn from tail vein of mice and analyzed by the *Pig-A* gene mutation assay. All mice were housed individually under specific pathogen-free conditions, with a 12 h light-dark cycle at the animal facility of NIHS. All mice were given tap water and gamma-ray irradiated CRF-1 pellets (Oriental Yeast Co., ltd.) *ad libitum*. Animal experiments were humanely conducted under the regulation and permission of the Animal Care and Use Committee of the National Institute of Health Sciences, Tokyo, Japan.

Antibodies: Anti-mouse TER119 antibody for erythroid cells staining (clone TER-119, PE-Cy7-conjugated) and anti-mouse CD24 antibody (clone M1/69, FITC-conjugated) were obtained from BioLegend.

***Pig-A* gene mutation assay in mice:** Mice *Pig-A* gene mutation assay was performed as previously described (5,8), with some modifications. In brief, EDTA/2K was dissolved in distilled water to make a 12% solution, and used as an anticoagulant. Eighteen μL of peripheral blood were mixed with 2 μL of EDTA solution. Two μL of blood/EDTA mixture was suspended in 0.2 mL of PBS, and the cells were labeled with 1 μg of each anti-mouse TER119 and anti-mouse CD24 antibodies. After incubation for 1 h in the dark at room temperature, the cells were washed once by centrifugation ($500 \times g$, 5 min), resuspended in 2 mL of PBS, and examined using a FACS Canto II flow cytometer (BD Biosciences). After gating for single cells, about 1,000,000 TER119-positive cells were analyzed for the presence of CD24 on their surface. The data were statistically compared with the corresponding solvent control using the Student's t-test.

Results

***Pig-A* gene mutation assay with mice peripheral blood:** Recent works provided that the erythrocyte-based *Pig-A* gene mutation assay is applicable across species (5–8). According to these reports, we modified the original *Pig-A* gene mutation assay and performed it with mice peripheral blood. To classify white blood cells (WBCs) and red blood cells (RBCs) in mice peripheral blood, RBCs were stained with anti-TER119 antibody. Anti-CD24 antibody was used to detect GPI-anchored protein as previously reported (8,10). The gating strategy that was used to score GPI anchor deficient RBCs population was shown in Fig. 1. Single cells including RBCs and WBCs were gated by light scatter (Fig. 1A). To exclude WBCs from this population, TER119-positive cells (Fig. 1B) were analyzed further for the presence on the cell surface of either the GPI-anchored CD24 (Fig. 1C and 1D). The gate used for CD24-negative cells was established by blood cell samples prepared without the fluorescent reagents.

***In vivo* genotoxicity tests on fullerene (C_{60}) analyzed by the *Pig-A* gene mutation assay:** At 2 and 8 weeks after the injection of C_{60} (3 mg/head) and ENU, we analyzed CD24-negative and -positive RBCs in peripheral blood. At both 2 and 8 weeks after the injection, higher amounts of CD24 deficient RBCs were observed in the ENU treated mice (Fig. 1D) as compared with the solvent control (not shown) and C_{60} treated mice (Fig. 1C), respectively. Frequencies of CD24-negative RBCs were summarized in Fig. 2. Frequency of CD24-negative RBCs was significantly increased in ENU treated mice (2 weeks after treatment; $30.12 \pm 3.54 \times 10^{-6}$, and 8 weeks after treatment; $36.64 \pm 15.71 \times 10^{-6}$). However, we detected no obvious differences in frequency of CD24-negative RBCs between C_{60} treated and non-treated mice ($0.25 \pm 0.30 \times 10^{-6}$ versus $0.42 \pm 0.19 \times 10^{-6}$ after 2 weeks and $0.82 \pm 0.54 \times 10^{-6}$ versus $1.87 \pm 1.51 \times 10^{-6}$ after 8 weeks).

These results indicated that although the *Pig-A* gene mutation assay with mouse peripheral blood was appropriately performed, C_{60} was negative for genotoxicity *in vivo* in the RBCs assessed in our study.

Discussion

We demonstrated here that C_{60} (3 mg/head) given intraperitoneally to male C57BL/6Cr mice was negative in the *Pig-A* gene mutation assay using peripheral blood, suggesting that C_{60} was not mutagenic to erythroid precursor cells or hematopoietic stem cells.

The *Pig-A* gene mutation assay is based on detections of GPI-anchored protein on the cell surface of RBCs. The *Pig-A* gene is involved in the synthesis of GPI anchors that link various protein markers to the cell surface. It is known that paroxysmal nocturnal hemoglobinuria (PNH) is caused by somatic *PIG-A* mutations in hematopoietic stem cells (HSCs) and Aerolysin-resistant HSCs from a patient with PNH exhibited clonal *PIG-A* mutations (11,12). Additionally, it is considered that the absence of GPI-anchored protein of RBCs is caused by mutations occurred in the *Pig-A* gene of nucleated erythroid precursors and/or of HSCs (6). These observations suggested that expression of GPI-anchored CD24 of RBCs is depending on the *Pig-A* gene mutations happened in erythroid precursors and/or of HSCs in bone marrows. According to this, we considered that our results, shown here using peripheral blood of mice, reflected genotoxicity of C_{60} on bone marrows.

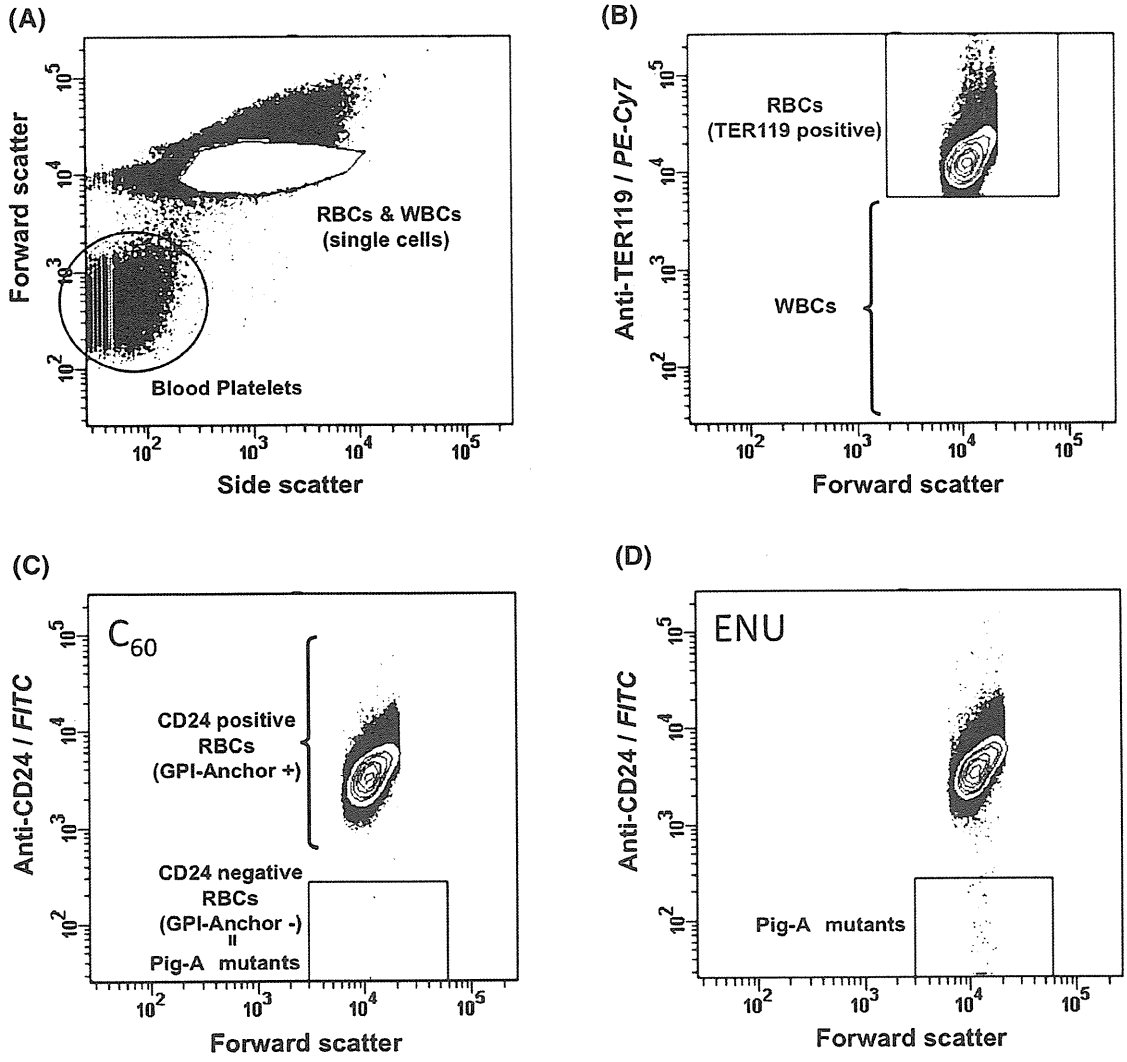

Fig. 1. Analysis of mouse peripheral blood by flow cytometry. (A) Single cell populations were gated and further analyzed with anti-TER119 antibody. (B) TER119-negative white blood cells were excluded from the gated single cell population. TER119-positive red blood cells (RBCs) were gated and further analyzed with anti-CD24 antibody. (C) Approximately 1×10^6 TER119-positive RBCs were analyzed for CD24 expression. CD24-negative RBCs (GPI-Anchor -) were scored as *Pig-A* mutants. In here, there were no obvious features in RBCs derived from C_{60} treated mice. (D) TER119-positive cells derived from ENU-treated mice were analyzed for CD24 expression.

Our data are consistent with the finding that C_{60} administered by gavage to ICR mice is negative in the *in vivo* bone marrow micronucleus test (4). These reports and our result suggest that intraperitoneal injection and gavage of C_{60} are negative for genotoxicity on bone marrow cells including erythroid precursors and HSCs. In both studies, however, the bone marrow was not exposed to C_{60} directly. A recent report showed that intratracheal instillation of C_{60} increased both mutation frequency (*gpt* assay) and DNA damage (comet assay) in the lung (3). From the mutation spectra, it was suggested that oxidative DNA damage might be involved in mutagenicity of C_{60} (3). C_{60}-phagocytized macrophages and granulomatous formations were also observed in the lung (3). Additionally, intratracheal instillation of C_{60} could induce inflammatory responses in the lung (13). It is known that reactive oxygen species (ROS) generation by nanoparticles could be due to particle-cell interactions, especially in the lungs where there is a rich pool of ROS producers like the inflammatory phagocytes, neutrophols and macrophages (14). According to these observations, it is possible that both direct exposure to the target tissue and inflammatory response are important factors in the evaluation of the genotoxicity of C_{60}.

On the other hand, details of inflammatory responses were unclear, but intraperitoneal application of C_{60} induced no obvious change on exposed area except for black patchy deposits on the serosal surfice in $p53^{+/-}$ mouse (1). Therefore it is expected that ROS generation

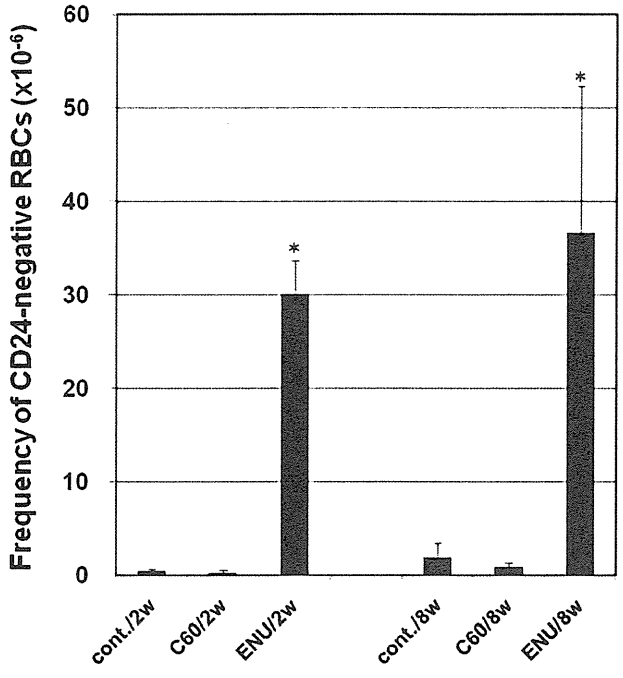

Fig. 2. Frequency of CD24-negative RBCs. At 2 and 8 weeks after mice were treated with C_{60} (3 mg/animal), ENU (40 mg/kg), or solvent, peripheral blood was withdrawn from the tail vein and RBCs were analyzed by flow cytometry for CD24 expression. Values are the mean ± SD of data from 6 animals (C_{60} and solvent) or 5 animals (ENU). *P*-values less than 0.0005 are indicated by asterisks.

by inflammatory responses might not occur and we detected negative genotoxicity in our case.

Recent reports including our results about genotoxicity of C_{60} are discrepant. However, it is known that C_{60} have an ability to quench and generate ROS (15,16). These discrepancies about genotoxicity of C_{60} may be caused by a duality of C_{60} itself. At this time, we cannot explain the mechanism(s) of C_{60} genotoxicity in detail, but we suspect that it is complex and includes oxidative DNA damages, inflammation, and other biological factors. To assess the genotoxicity of C_{60} more fully, we need a comprehensive whole body survey.

Acknowledgement: This work was supported by Health and Labor Sciences Research Grant, Japan, Grant Number: H21-chemical-general-008, and Human Science Foundation, Japan; Grant Number: KHB1006.

References

1 Takagi A, Hirose A, Nishimura T, Fukumori N, Ogata A, Ohashi N, Kitajima S, Kanno J. Induction of mesothelioma in p53$^{+/-}$ mouse by intraperitoneal application of multi-wall carbon nanotube. J Toxicol Sci. 2008; 33: 105-16.

2 Sakamoto Y, Nakae D, Fukumori N, Tayama K, Maekawa A, Imai K, Hirose A, Nishimura T, Ohashi N, Ogata A. Induction of mesothelioma by a single intrascrotal administration of multi-wall carbon nanotube in intact male Fischer 344 rats. J Toxicol Sci. 2009; 34: 65-76.

3 Totsuka Y, Higuchi T, Imai T, Nishikawa A, Nohmi T, Kato T, Masuda S, Kinae N, Hiyoshi K, Ogo S, Kawanishi M, Yagi T, Ichinose T, Fukumori N, Watanabe M, Sugimura T, Wakabayashi K. Genotoxicity of nano/microparticles in *in vitro* micronuclei, *in vivo* comet and mutation assay systems. Part Fibre Toxicol. 2009; 6: 23.

4 Shinohara N, Matsumoto K, Endoh S, Maru J, Nakanishi J. *In vitro* and *in vivo* genotoxicity tests on fullerene C_{60} nanoparticles. Toxicol Lett. 2009; 191: 289-96.

5 Miura D, Dobrovolsky VN, Kasahara Y, Katsuura Y, Heflich RH. Development of an *in vivo* gene mutation assay using the endogenous *Pig-A* gene: I. Flow cytometric detection of CD59-negative peripheral red blood cells and CD48-negative spleen T-cells from the rat. Environ Mol Mutagen. 2008; 49: 614-21.

6 Miura D, Dobrovolsky VN, Mittelstaedt RA, Kasahara Y, Katsuura Y, Heflich RH. Development of an *in vivo* gene mutation assay using the endogenous *Pig-A* gene: II. Selection of *Pig-A* mutant rat spleen T-cells with proaerolysin and sequencing *Pig-A* cDNA from the mutants. Environ Mol Mutagen. 2008; 49: 622-30.

7 Dobrovolsky VN, Shaddock JG, Mittelstaedt RA, Manjanatha MG, Miura D, Uchikawa M, Mattison DR, Morris SM. Evaluation of Macaca mulatta as a model for genotoxicity studies. Mutat Res. 2009; 673: 21-8.

8 Phonethepswath S, Bryce SM, Bemis JC, Dertinger SD. Erythrocyte-based *Pig-a* gene mutation assay: demonstration of cross-species potential. Mutat Res. 2008; 657: 122-6.

9 Miura D, Dobrovolsky VN, Kimoto T, Kasahara Y, Heflich RH. Accumulation and persistence of *Pig-A* mutant peripheral red blood cells following treatment of rats with single and split doses of *N*-ethyl-*N*-nitrosourea. Mutat Res. 2009; 677: 86-92.

10 Keller P, Tremml G, Rosti V, Bessler M. X inactivation and somatic cell selection rescue female mice carrying a Piga-null mutation. Proc Natl Acad Sci U S A. 1999; 96: 7479-83.

11 Takeda J, Miyata T, Kawagoe K, Iida Y, Endo Y, Fujita T, Takahashi M, Kitani T, Kinoshita T. Deficiency of the GPI anchor caused by a somatic mutation of the *PIG-A* gene in paroxysmal nocturnal hemoglobinuria. Cell. 1993; 73: 703-11.

12 Hu R, Mukhina GL, Piantadosi S, Barber JP, Jones RJ, Brodsky RA. *PIG-A* mutations in normal hematopoiesis. Blood. 2005; 105: 3848-54.

13 Park EJ, Kim H, Kim Y, Yi J, Choi K, Park K. Carbon fullerenes (C_{60}s) can induce inflammatory responses in the lung of mice. Toxicol Appl Pharmacol. 2010; 244: 226-33.

14 Li JJ, Muralikrishnan S, Ng CT, Yung LY, Bay BH. Nanoparticle-induced pulmonary toxicity. Exp Biol Med (Maywood). 2010; 235: 1025-33.

15 Markovic Z, Trajkovic V. Biomedical potential of the reactive oxygen species generation and quenching by

fullerenes (C_{60}). Biomaterials. 2008; 29: 3561-73.
16 Singh N, Manshian B, Jenkins GJ, Griffiths SM, Williams PM, Maffeis TG, Wright CJ, Doak SH. NanoGenotoxicology: the DNA damaging potential of engineered nanomaterials. Biomaterials. 2009; 30: 3891-914.

Food and Chemical Toxicology 49 (2011) 1298–1302

Contents lists available at ScienceDirect

Food and Chemical Toxicology

journal homepage: www.elsevier.com/locate/foodchemtox

Lack of promoting effect of titanium dioxide particles on ultraviolet B-initiated skin carcinogenesis in rats

Jiegou Xu[a,e], Yoko Sagawa[b], Mitsuru Futakuchi[a], Katsumi Fukamachi[a], David B. Alexander[a,e], Fumio Furukawa[c], Yoshiaki Ikarashi[d], Tadashi Uchino[d], Tetsuji Nishimura[d], Akimichi Morita[b], Masumi Suzui[a], Hiroyuki Tsuda[e,*]

[a] Department of Molecular Toxicology, Nagoya City University Graduate School of Medical Sciences, 1-Kawasumi, Mizuho-cho, Mizuho-ku, Nagoya 467-8601, Japan
[b] Department of Dermatology, Nagoya City University Graduate School of Medical Sciences, 1-Kawasumi, Mizuho-cho, Mizuho-ku, Nagoya 467-8601, Japan
[c] Daiyukai Institute of Medical Science,Inc., 64 Goura, Nishiazai, Azai-cho, Ichinomiya 491-0113, Japan
[d] National Institute of Health Sciences, 1-18-1 Kamiyoga, Setagaya-ku, Tokyo 158-8501, Japan
[e] Laboratory of Nanotoxicology Project, Nagoya City University, 3-1 Tanabedohri, Mizuho-ku, Nagoya 467-8603, Japan

ARTICLE INFO

Article history:
Received 15 October 2010
Accepted 9 March 2011
Available online 15 March 2011

Keywords:
TiO_2
Nano-size
Skin
Mammary gland
Carcinogenesis
UVB

ABSTRACT

Titanium dioxide (TiO_2) is used in sunscreens and cosmetics as an ultraviolet light screen. TiO_2 has carcinogenic activity in the rat lung, but its effect on the skin has not been reported. We examined the promoting/carcinogenic effect of nano-size TiO_2 particles using a two-stage skin model. c-Ha-*ras* proto-oncogene transgenic (H*ras*128) rats, which are sensitive to skin carcinogenesis, and their wild-type siblings were exposed to ultraviolet B radiation on shaved back skin twice weekly for 10 weeks; then the shaved area was painted with a 100 mg/ml TiO_2 suspension twice weekly until sacrifice. All rats were killed at week 52 except for female H*ras*128 rats which were sacrificed at week 16 because of early mammary tumor development. Skin tumors developed in male H*ras*128 rats and mammary tumors developed in both sexes of H*ras*128 rats and in wild-type female rats, but tumor incidence was not different from controls. TiO_2 particles were detected in the upper stratum corneum but not in the underlying skin tissue layers. TiO_2 particles also did not penetrate a human epidermis model *in vitro*. Our data suggest that TiO_2 does not cause skin carcinogenesis, probably due to its inability to penetrate through the epidermis and reach underlying skin structures.

1. Introduction

Titanium dioxide (TiO_2) is a wide spectrum physical sunscreen (Anderson et al., 1997) and is used in sunscreen formulations to protect against UV radiation-related skin lesions (Gelis et al., 2003; Rouabhia et al., 2002; Suzuki, 1987). TiO_2 nanoparticles have been introduced into sunscreen and cosmetics formulations recently to improve their physical properties, e.g., make them more transparent and less viscous, without losing their UV light blocking ability (Newman et al., 2009). Nanoparticles, defined as having at least one dimension of 100 nm or less (ISO, 2008), were postulated to be able to penetrate the stratum corneum and diffuse into underlying skin structures, which gives rise to concerns about potential health risks (Newman et al., 2009; Nohynek et al., 2008). In human skin samples, topically applied tetramethylammonium hydroxide nanoparticles and sodium bis(2-ethylhexyl) sulfosuccinate nanoparticles get into the hair follicles and the stratum corneum and reach the viable epidermis (Baroli et al., 2007). Dermally administrated near-infrared quantum dot nanoparticles can localize, possibly via skin macrophages and Langerhans cells, to regional lymph nodes (Kim et al., 2004). These findings and the report that endothelial cells have the capacity to internalize nanoparticles (Peters et al., 2004) suggests the possibility of potential pro-inflammatory, cytotoxic or other harmful effects.

TiO_2 particles including micro- and nano-sized, are evaluated as a Group 2B carcinogen by WHO/International Agency for Research on Cancer (IARC) (Baan et al., 2006), based on 2-year animal aerosol inhalation studies (Lee et al., 1985; Pott and Roller, 2005). The mechanism of lung carcinogenesis involves MIP1α derived from TiO_2-laden alveolar macrophages (Xu et al., 2010). Therefore, it is possible that TiO_2 particles may be carcinogenic to the skin and subcutaneous tissues if they penetrate into the epidermis and cause inflammatory lesions, including enhanced macrophage

Abbreviations: TiO_2, titanium dioxide; H*ras*128 rat, human c-Ha-*ras* proto-oncogene transgenic rat; UVB, ultraviolet B light.

* Corresponding author. Tel.: +81 52 836 3496; fax: +81 52 836 3497.
E-mail address: htsuda@med.nagoya-cu.ac.jp (H. Tsuda).

0278-6915/$ - see front matter © 2011 Elsevier Ltd. All rights reserved.
doi:10.1016/j.fct.2011.03.011

activity. Consequently, an important issue is whether TiO_2 particles have the ability to penetrate the stratum corneum and reach the epidermis. Pflucker et al. and Mavon et al. reported that when TiO_2 particles, including micro- and nano-sizes, were topically applied repeatedly to human skin samples *in vitro*, only the upper stratum corneum and hair follicles showed any evidence of particle penetration (Mavon et al., 2007; Pflucker et al., 2001). Even in human skin samples after tape stripping, ultrafine TiO_2 did not penetrate beyond the stratum corneum (Gottbrath and Muller-Goymann, 2003). These results suggest that dermal penetration of TiO_2 particles is in fact associated with hair follicle orifice and not due to direct diffusion through the stratum corneum into the epidermis. Contrary to these *in vitro* findings, Wu et al. reported that TiO_2 nanoparticles could penetrate through the stratum corneum and be located in the deep layer of the epidermis after being topically applied to pig ear *in vivo* for 30 days (Wu et al., 2009). This study also reported that TiO_2 nanoparticles reached different tissues and induced diverse pathological lesions in several major organs after 60 days dermal exposure to hairless mice. The difference in skin penetration between *in vitro* and *in vivo* topical application of TiO_2 particles needs further investigation.

Here, we report results of the carcinogenic effect of TiO_2 particles in the skin using a UVB-initiated 2-stage carcinogenesis protocol. For this purpose, human c-Ha-*ras* proto-oncogene transgenic rats (H*ras* 128) were used because they are more sensitive to chemically induced skin carcinogens than wild-type rats (Park et al., 2004). Our data indicate that TiO_2 did not penetrate through the epidermis and reach the underlying skin structures and did not have skin carcinogenic activity.

2. Materials and methods

2.1. Animals

Transgenic rats carrying the human c-Ha-ras proto-oncogene (H*ras*128 rats), known to be sensitive to chemically induced skin carcinogenesis in males and mammary carcinogenesis in females, and their wild-type counterparts were maintained and bred by CLEA Japan Co., Ltd. (Tokyo, Japan). The animals were housed in the Animal Center of Nagoya City University Medical School and maintained on a 12 h light/12 h dark cycle and received Oriental MF basal diet (Oriental Yeast Co., Tokyo, Japan) and water *ad libitum*. The study was conducted according to the Guidelines for the Care and Use of Laboratory Animals of Nagoya City University Medical School and the experimental protocol was approved by the Institutional Animal Care and Use Committee (H17-28).

2.2. Preparation of titanium dioxide suspension

Ultrafine grade TiO_2 particles (CAS No. 13463-67-7, rutile type, without coating, mean primary diameter of 20 nm, Ishihara Sangyo Kaisha, Ltd., Osaka, Japan) were provided by Japan Cosmetic Association, Tokyo, Japan. TiO_2 particles were suspended at 100 mg/ml in Pentalan 408 (pentaerythritol tetraethylhexanoate, CAS 7299-99-2, Nikko Chemicals Co., Tokyo, Japan). The suspensions were sonicated for 30 min just before use, since TiO_2 particles are known to form aggregates. The size distribution of the TiO_2 suspension in Pentalan 408 was analyzed by a Particle Size Distribution Analyzer (Shimadzu Techno-Research, Inc. Kyoto, Japan.

2.3. Promotion study in the skin

A total of 80 H*ras*128 rats and their wild-type siblings, of both sexes and aged 10 weeks old, were randomly allocated to three groups after a 1 week acclimation: Group 1 received ultraviolet B (UVB) radiation (UVB radiation unit, Dermaray 100, Eisai-Toshiba, Tokyo, Japan) 2 times per week for 10 weeks at 800 mJ/cm^2, 7 min, 20 cm distance from the shaved target skin, followed by painting with 0.5 ml of TiO_2 suspended in Pentalan 408 at 100 mg/ml on the shaved area twice a week until sacrifice. Group 2 received UVB radiation and painting with the vehicle Pentalan 408 on the shaved area twice a week until sacrifice, and Group 3 received painting with 0.5 ml of TiO_2 suspension as in Group1 but without prior UVB radiation. The painting was done gently using a bacterial spreader. The hair of the back was cut in a 3 × 3 cm area with an electric clipper and the remaining hairs were thoroughly shaved with a razor just before every UVB irradiation and/or TiO_2 painting. Any grossly visible papilloma lesions were carefully examined every day (Fig. 1). All the animals were sacrificed at week 52 (after 42 weeks painting) except for the female H*ras*128 rats which were terminated at week 16 (after 6 weeks painting) due to early mammary tumor development. The organs, the skin, brain, lung, liver, mammary gland, mesenterial lymph nodes, spleen and kidney, were excised and fixed in 4% paraformaldehyde solution in PBS buffer adjusted to pH 7.3 and processed for light microscopic examination.

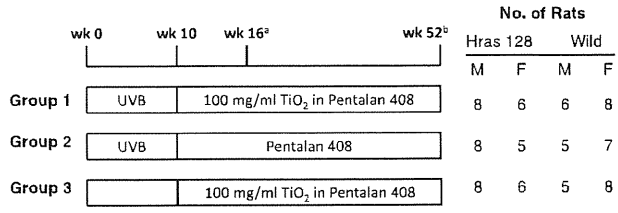

Fig. 1. Schematic of the treatment schedule used to test for skin carcinogenesis in rats. Rats were randomly allocated into three groups: Group 1: UVB radiation for 10 weeks, followed by painting with TiO_2 suspension twice a week; Group 2: UVB radiation for 10 weeks, followed by painting with the vehicle, Pentalan 408, twice a week; and Group 3: painting with TiO_2 suspension twice a week without previous UVB radiation. (a) male H*ras*128 rats and male and female wild-type rats were sacrificed at week 52 and (b) female H*ras*128 rats were sacrificed at week 16 due to early mammary tumor development.

2.4. In vitro TiO_2 penetration assay

To evaluate whether TiO_2 particles could penetrate into the epidermis, the 12 well LabCyte EPI-MODEL (Japan Tissue Engineering Co., Ltd, Aichi, Japan) was used. Eight wells were exposed to either 43.2 μl of Pentalan 408 alone or 100 or 200 mg/ml of TiO_2 suspended in Pentalan 408 for 48 h. The 24 samples in the receiving chambers were then collected for detection of elemental titanium.

2.5. Determination of the elemental titanium

For the detection of elemental titanium, 1 ml of the medium collected from the receiving chambers was treated with 5 ml concentrated HNO_3 for 22 min in a microwave oven. Titanium in the treated solutions was determined by inductively coupled plasma/mass spectrometry (ICP-MS) (HP-4500, Hewlett-Packard Co., Houston, Texas) under the following conditions: RF power-1450 W; RF refraction current-5 W; Plasma gas current-15 L/min; Carrier gas current-0.91 L/min; Peri pump-0.2 rps; Monitoring mass-m/z 48 (Ti); Integrating interval-0.1 s; Sampling period 0.31 s.

2.6. Cytokine analysis

Five wild-type male Sprague–Dawley rats aged 10 weeks were shaved as described above and painted with 0.5 ml of 100 mg/ml of TiO_2 suspended in Pentalan 408 on the shaved area once a day for 14 consecutive days. Five rats were painted with Pentalan 408 as the control. The painted area was excised, rinsed with cold PBS 3 times, and homogenized in 1 ml of T-PER, Tissue Protein Extraction Reagent (Pierce, Rockford, IL, USA), containing 1% (v/v) proteinase Inhibitor Cocktail (Sigma–Aldrich, St Louis, MO, USA). The homogenates were clarified by centrifugation at 10,000g for 5 min at 4 °C. Protein content was measured using a BCA™ Protein Assay Kit (Pierce). The levels of IL-1α, IL-1β, IL-6, GM-CSF, G-CFS, TNFα, IFNγ, IL-18, MCP1, MIP1α, GRO/KC, and VEGF were measured by Multiplex Suspension array (GeneticLab, Co., Ltd., Sapporo, Japan).

2.7. Statistical analysis

Statistical analysis was performed using the Kruskal–Wallis and Bonferroni/Dunn's multiple comparison tests. The statistical significance was analyzed using a two tailed Student's *t*-test and the Bonferroni/Dunn's multiple comparison tests. A P value of <0.05 was considered to be significant.

3. Results

3.1. Size analysis of TiO_2 particles

The size (diameter) of TiO_2 particles suspended in Pentalan 408 ranged from 10 nm to 300 μm, with a mean size of 4.967 ± 0.500 μm and a median size of 4.570 μm, indicating that a large majority of the original nano-size (ultrafine grade) TiO_2 particles formed aggregates in the Pentalan 408 suspension (Fig. 2).

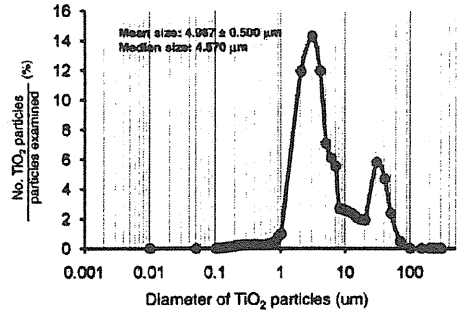

Fig. 2. Size distribution of TiO_2 suspended in Pentalan 408. The size distribution of TiO_2 particles suspended in Pentalan 408 was analyzed by a Particle Size Distribution Analyzer. The mean size was 4.967 ± 0.500 µm and the median size and 4.570 µm.

3.2. Incidence of skin and mammary tumors

In male H*ras*128 rats, papillomas on the back skin developed from week 32 and the incidence of skin papillomas was 1 out of 8 in Groups 1 and Group 3. No skin tumors were observed on the targeted back skin in female H*ras*128 rats or wild-type rats of either sex. Eye lid squamous cell papillomas were found in wild-type female rats exposed to UVB (Groups 1 and 2) with incidences of 12.5% and 14.3% (Table 1). No statistically significant inter-group differences in incidence, multiplicity or weight were found (Table 1).

Mammary tumors, diagnosed as adenocarcinomas, were induced with high incidence in H*ras*128 rats of both sexes. Wild-type female rats also had a relatively high incidence of mammary tumors compared with historical controls of spontaneous mammary tumor development. No statistically significant inter-group differences in incidence, multiplicity or weight were observed (Table 2).

3.3. Tissue analysis of TiO_2 particles

In the rat skin, no inflammatory lesions were observed by histopathological examination. TiO_2 aggregates of various sizes were observed in the upper stratum corneum, but TiO_2 was not found in the underlying epidermis, dermis or subcutaneous tissue (Fig. 3A). Some particles were found in the hair follicles at the level of the granular cell layer in all the TiO_2 treated groups, but not in the deeper parts of the hair follicles or in the surrounding tissue.

In the human epidermis model, TiO_2 aggregates were observed only on the cornified layer of the epidermis, but not in the epidermis (Fig. 3B). The amount of elemental titanium in the receiving chamber did not show any significant difference from the vehicle alone group (Fig. 3C).

Table 2
Mammary tumors in Hras128 and wild-type rats

Sex	Group	Treatment	Incidence[a] (%)	Multiplicity[a] (No./rat)	Weight[a] (g/rat)
Hras128					
Male	1	UVB + TiO_2	4/8 (50)	0.50 ± 0.53	10.50 ± 19.56
	2	UVB	3/8 (36)	0.38 ± 0.51	10.17 ± 17.69
	3	TiO_2	4/8 (50)	0.50 ± 0.53	6.33 ± 14.16
Female	1	UVB + TiO_2	5/6 (83)	1.67 ± 1.37	11.48 ± 20.61
	2	UVB	2/5 (40)	0.60 ± 0.89	0.28 ± 0.53
	3	TiO_2	6/6 (100)	1.33 ± 0.52	4.49 ± 9.76
Wild-type					
Male	1	UVB + TiO_2	0/6	0	0
	2	UVB	0/5	0	0
	3	TiO_2	0/5	0	0
Female	1	UVB + TiO_2	1/8(12.5)	0.13 ± 0.35	0.63 ± 1.80
	2	UVB	1/7(14.3)	0.14 ± 0.38	0.73 ± 1.93
	3	TiO_2	0/8(0)	0	0

[a] Rats died before sacrifice at week 52 were included.

3.4. Cytokine analysis of the rat skin tissue

The levels of 12 inflammatory cytokines (IL-1α, IL-1β, IL-6, GM-CSF, G-CFS, TNFα, IFNγ, IL-18, MCP1, MIP1α, GRO/KC, and VEGF) in the skin of rats receiving TiO_2 treatment is shown in Table 3. TiO_2 treatment did not have a significant effect on the expression of the cytokine levels in the skin compared with the vehicle group.

4. Discussion

TiO_2 particles, nano- and larger scale, are known to be carcinogenic to the rat lung (Baan et al., 2006), and the mechanism of lung carcinogenesis involves MIP1α derived from TiO_2-laden alveolar macrophages (Xu et al., 2010). Thus, they are deemed to have the potential to cause skin tumors after long-term topical application,

Table 1
Skin tumors in Hras128 rats and wild-type rats

Sex	Group	Treatment	Total No. of rats (died before termination)	Survival time (mean week ± SD)	Skin tumor[a]	
					Incidence (%)	Multiplicity (No./rat)
Hras128						
Male	1	UVB + TiO_2	8 (4[b])	47.3 ± 6.8	1/8 (12.5)	0.13 ± 0.35
	2	UVB	8 (4[b])	48.4 ± 5.5	0/8	0
	3	TiO_2	8 (3[b])	48.9 ± 4.7	1/8 (12.5)	0.13 ± 0.35
Female	1	UVB + TiO_2	6	16	0/6	0
	2	UVB	5	16	0/5	0
	3	TiO_2	6	16	0/6	0
Wild-type						
Male	1	UVB + TiO_2	6	52	0/6	0
	2	UVB	5	52	0/5	0
	3	TiO_2	5	52	0/5	0
Female	1	UVB + TiO_2	8 (1[c,d])	51.4 ± 1.8	1/8 (12.5)	0.13 ± 0.35
	2	UVB	7 (1[c],1[d])	51.4 ± 1.5	1/7 (14.3)	0.14 ± 0.38
	3	TiO_2	8	52	0/8	0

[a] Rats died before sacrifice at week 52 were included in statistic calculation of the incidence and multiplicity.
[b] Rats died of mammary tumors between week 33 and week 51.
[c] Rats died of eye lid skin tumors during week 48 and week 50.
[d] Rats died of mammary tumors during week 48.

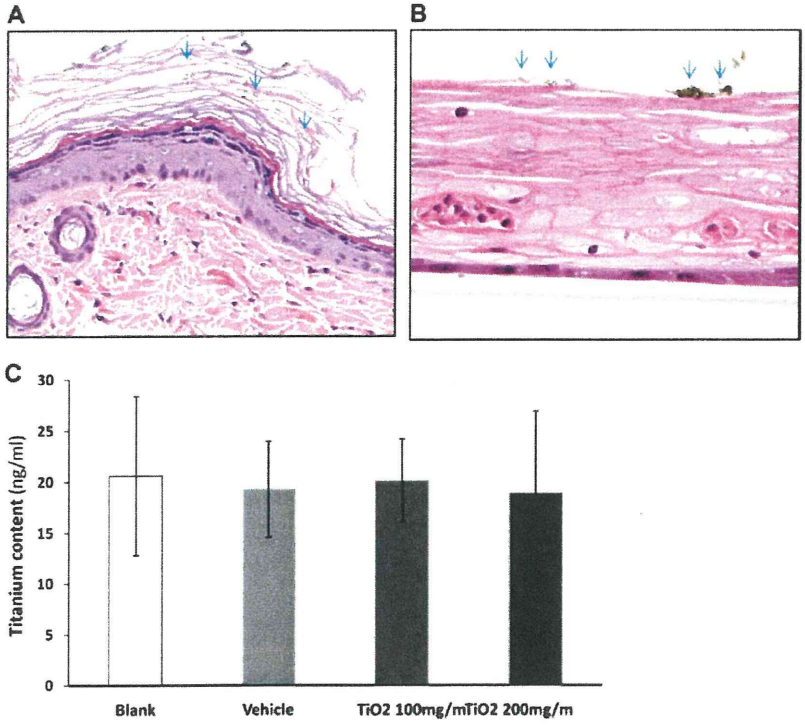

Fig. 3. TiO_2 particles did not penetrate the epidermis. (A) TiO_2 aggregates were observed in the upper stratum corneum, but were not found in the underlying epidermis, dermis or subcutaneous tissue. (B) in the *in vitro* penetration assay, TiO_2 aggregates were localized on the top of the human epidermis model, but not within the epidermis. (C) the amount of elemental titanium detected in the receiving chambers is expressed as mean ± SD. A total of 24 wells of the epidermis model were exposed to the vehicle, 100 mg/ml or 200 mg/ml TiO_2 suspension. Arrows indicate TiO_2 aggregates.

Table 3
Expression level of 12 inflammatory cytokines in the skin treated with Petalan 408 or TiO_2 (5 rats in each group, ng/mg protein)

Cytokine	Pentalan 408	TiO_2 suspension
GM-CSF	23.65 ± 36.48	23.01 ± 16.75
G-CSF	0.37 ± 0.21	0.13 ± 0.16
IL-1α	2914 ± 433	3176 ± 785
IL-1β	38.81 ± 7.49	30.87 ± 7.26
IL-6	1.33 ± 2.97	0.00 ± 0.00
TNFα	29.56 ± 7.75	26.00 ± 8.07
INFγ	5.91 ± 0.68	4.70 ± 1.10
IL-18	845 ± 234	763 ± 299
MCP-1	90 ± 125	123 ± 125
MIP-1α	3.47 ± 7.75	0.00 ± 0.00
GRO/KC	82.66 ± 21.86	63.04 ± 28.76
VEGF	17.96 ± 19.05	14.04 ± 17.55

especially if they induce inflammatory lesions including enhanced macrophage activity in the skin. The present study is the first report of an *in vivo* skin promotion/carcinogenesis study of TiO_2 particles topically applied to the back skin of rats. The incidence of skin tumors in male H*ras*128 was 1 out of 8 (12.5%) in the TiO_2 alone group and in the UVB plus TiO_2 group, higher than that of spontaneously developed skin tumors in these rats (less than 5%) (Park et al., 2004). However, no inter-group difference was observed. Our results demonstrate that TiO_2 suspension does not have a promoting effect on skin carcinogenesis after UVB radiation.

The lack of skin carcinogenesis promotion activity is probably due to lack of penetration of TiO_2 particles through the epidermis to the dermis, where skin tumors arise. Histologically, topically applied TiO_2 particles were located only in the upper stratum corneum and in some hair follicles at the level of granular cell layer, but were not found in the epidermis or the underlying dermis. Our results are consistent with other reports (Mavon et al., 2007; Pflucker et al., 2001). Furthermore, results of the *in vitro* skin model assay used in our study indicate that TiO_2 particles do not penetrate the human epidermis. Since the size of TiO_2 particles was a mixture of nano-size and micro-size, the results indicate that overall the particles do not penetrate through the epidermis and cause an inflammatory response in the skin, although a trace amount of nano-size particles might penetrate the skin tissue. In our study, a large majority of the original nano-size TiO_2 particles (ultrafine grade) formed micro-size aggregates in the Pentalan 408 suspension and this may have affected the particle penetration. The difference between the report of Wu et al. (2009) and ours *in vivo* observation may be ascribed to different test animals, different TiO_2 particles used or different methods of making the TiO_2 particle suspension.

The high incidence of mammary tumors H*ras*128 rats regardless of treatment is attributed to spontaneous development, which is specific to the H*ras*128 rat (Asamoto et al., 2000; Matsuoka et al., 2007; Tsuda et al., 2005).

TiO_2 particle-induced lung carcinogenesis in rats is due to chronic inflammation (ILSI, 2000) with the cytokine MIP1α, derived from TiO_2-laden alveolar macrophages, being an important mediator of carcinogenesis (Xu et al., 2010). In the present study, analysis of 12 inflammatory cytokines, IL-1α, IL-1β, IL-6, GM-CSF, G-CFS, TNFα, IFNγ, IL-18, MCP1, MIP1α, GRO/KC, and VEGF, indicated that no significant change in the expression level of these cytokines occurred after topical application of TiO_2. This result, together with histological observation, indicates that no inflammatory reaction is evoked by topical application of TiO_2. This may partly explain why topical application of TiO_2 suspension has no carcinogenic effect in the skin.

Since tumor promotion activity is considered to be a weak carcinogenic activity (IARC, 1980; Ito et al., 1988, 2003; Konishi et al.,

1987; Nishikawa et al., 1994; Peraino et al., 1971; Pitot et al., 1978; Yamanaka et al., 1996), lack of promotion activity can be interpreted as lack of carcinogenic activity. Thus, the results of our present study indicate that topical application of TiO_2 suspension does not have carcinogenic activity on UVB-treated skin in rats, probably due to lack of penetration through the epidermis. In conclusion, our results indicate that topical application of TiO_2 can be considered to be safe and not carcinogenic to the skin or other organs.

5. Conflict of Interest

The authors declare that there are no conflicts of interest.

Acknowledgement

This work was supported by Health and Labour Sciences Research Grants (Research on Risk of Chemical Substance, H19-kagaku-ippan-006 and H22-kagaku-ippan-005), and Grant-in aid for cancer research from the Ministry of Health, Labour and Welfare, Japan, a grant-in-aid for the Second Term Comprehensive 10-year Strategy for Cancer Control from the Ministry of Health, Labour and Welfare, Japan, and grants-in aid for Cancer Research from the Ministry of Education, Culture, Sports, Science and Technology. Jiegou Xu was a recipient of Bantane Houtokukai Fellowship when this study was performed.

References

Anderson, M., Hewitt, J., Spruce, J., 1997. Broad-spectrum physical sunscreen: titanium dioxide and zinc oxide. In: Lowe, N.J., Shaath, N.A., MA, P. (Eds.), Sunscreens: Development. Evaluation and Regulatory Aspects, New York, Dekker, pp. 357–397.

Asamoto, M., Ochiya, T., Toriyama-Baba, H., Ota, T., Sekiya, T., Terada, M., Tsuda, H., 2000. Transgenic rats carrying human c-Ha-ras proto-oncogenes are highly susceptible to *N*-methyl-*N*-nitrosourea mammary carcinogenesis. Carcinogenesis 21, 243–249.

Baan, R., Straif, K., Grosse, Y., Secretan, B., El Ghissassi, F., Cogliano, V., 2006. Carcinogenicity of carbon black, titanium dioxide, and talc. Lancet Oncol. 7, 295–296.

Baroli, B., Ennas, M.G., Loffredo, F., Isola, M., Pinna, R., Lopez-Quintela, M.A., 2007. Penetration of metallic nanoparticles in human full-thickness skin. J. Invest. Dermatol. 127, 1701–1712.

Gelis, C., Girard, S., Mavon, A., Delverdier, M., Paillous, N., Vicendo, P., 2003. Assessment of the skin photoprotective capacities of an organo-mineral broad-spectrum sunblock on two ex vivo skin models. Photodermatol. Photoimmunol. Photomed. 19, 242–253.

Gottbrath, S., Muller-Goymann, C.C., 2003. Penetration and visualization of titanium dioxide microparticles in human stratum corneum-effect of different formulations on the penetration of titanium dioxide. SOFW J. 129, 11–17.

IARC (1980). Long-term and short-term screening assays for carcinogens: a critical appraisal, 1980/01/01 edn).

ILSI, 2000. The relevance of the rat lung response to particle overload for human risk assessment: a workshop consensus report. ILSI Risk Science Institute Workshop Participants. Inhal. Toxicol. 12, 1–17.

ISO (2008). Nanotechnologies-Terminology and definition for nano-objects-nanoparticle, nanofibre and nanoplate. ISO/TS 27687.

Ito, N., Imaida, K., Tsuda, H., Shibata, M., Aoki, T., de Camargo, J.L., Fukushima, S., 1988. Wide-spectrum initiation models: possible applications to medium-term multiple organ bioassays for carcinogenesis modifiers. Jpn. J. Cancer Res. 79, 413–417.

Ito, N., Tamano, S., Shirai, T., 2003. A medium-term rat liver bioassay for rapid in vivo detection of carcinogenic potential of chemicals. Cancer Sci. 94, 3–8.

Kim, S., Lim, Y.T., Soltesz, E.G., De Grand, A.M., Lee, J., Nakayama, A., Parker, J.A., Mihaljevic, T., Laurence, R.G., Dor, D.M., Cohn, L.H., Bawendi, M.G., Frangioni, J.V., 2004. Near-infrared fluorescent type II quantum dots for sentinel lymph node mapping. Nat. Biotechnol. 22, 93–97.

Konishi, Y., Yokose, Y., Mori, Y., Yamazaki, H., Yamamoto, K., Nakajima, A., Denda, A., 1987. Lung carcinogenesis by *N*-nitroso bis(2-hydroxypropyl)amine-related compounds and their formation in rats. IARC Sci. Publ. 1, 250–252.

Lee, K.P., Trochimowicz, H.J., Reinhardt, C.F., 1985. Pulmonary response of rats exposed to titanium dioxide (TiO_2) by inhalation for two years. Toxicol. Appl. Pharmacol. 79, 179–192.

Matsuoka, Y., Kawaguchi, H., Yoshida, H., Tsuda, H., Tsubura, A., 2007. Rat mammary preneoplasia and neoplasia: a model for human breast cancer research. Trends Cancer Res. 3, 1–13.

Mavon, A., Miquel, C., Lejeune, O., Payre, B., Moretto, P., 2007. In vitro percutaneous absorption and in vivo stratum corneum distribution of an organic and a mineral sunscreen. Skin Pharmacol. Physiol. 20, 10–20.

Newman, M.D., Stotland, M., Ellis, J.I., 2009. The safety of nanosized particles in titanium dioxide- and zinc oxide-based sunscreens. J. Am. Acad. Dermatol. 61, 685–692.

Nishikawa, A., Furukawa, F., Imazawa, T., Yoshimura, H., Ikezaki, S., Hayashi, Y., Takahashi, M., 1994. Effects of cigarette smoke on *N*-nitrosobis(2-oxopropyl)amine-induced pancreatic and respiratory tumorigenesis in hamsters. Jpn. J. Cancer Res. 85, 1000–1004.

Nohynek, G.J., Dufour, E.K., Roberts, M.S., 2008. Nanotechnology, cosmetics and the skin: is there a health risk? Skin Pharmacol. Physiol. 21, 136–149.

Park, C.B., Fukamachi, K., Takasuka, N., Han, B.S., Kim, C.K., Hamaguchi, T., Fujita, K., Ueda, S., Tsuda, H., 2004. Rapid induction of skin and mammary tumors in human c-Ha-ras proto-oncogene transgenic rats by treatment with 7, 12-dimethylbenz[a]anthracene followed by 12-O-tetradecanoylphorbol 13-acetate. Cancer Sci. 95, 205–210.

Peraino, C., Fry, R.J., Staffeldt, E., 1971. Reduction and enhancement by phenobarbital of hepatocarcinogenesis induced in the rat by 2-acetylaminofluorene. Cancer Res. 31, 1506–1512.

Peters, K., Unger, R.E., Kirkpatrick, C.J., Gatti, A.M., Monari, E., 2004. Effects of nano-scaled particles on endothelial cell function in vitro: studies on viability, proliferation and inflammation. J. Mater. Sci.: Mater. Med. 15, 321–325.

Pflucker, F., Wendel, V., Hohenberg, H., Gartner, E., Will, T., Pfeiffer, S., Wepf, R., Gers-Barlag, H., 2001. The human stratum corneum layer: an effective barrier against dermal uptake of different forms of topically applied micronised titanium dioxide. Skin Pharmacol. Appl. Skin Physiol. 14 (Suppl. 1), 92–97.

Pitot, H.C., Barsness, L., Goldsworthy, T., Kitagawa, T., 1978. Biochemical characterisation of stages of hepatocarcinogenesis after a single dose of diethylnitrosamine. Nature 271, 456–458.

Pott, F., Roller, M., 2005. Carcinogenicity study with nineteen granular dusts in rats. Eur. J. Oncol. 10, 249–281.

Rouabhia, M., Mitchell, D.L., Rhainds, M., Claveau, J., Drouin, R., 2002. A physical sunscreen protects engineered human skin against artificial solar ultraviolet radiation-induced tissue and DNA damage. Photochem. Photobiol. Sci. 1, 471–477.

Suzuki, M., 1987. Protective effect of fine-particle titanium dioxide on UVB-induced DNA damage in hairless mouse skin. Photodermatology 4, 209–211.

Tsuda, H., Fukamachi, K., Ohshima, Y., Ueda, S., Matsuoka, Y., Hamaguchi, T., Ohnishi, T., Takasuka, N., Naito, A., 2005. High susceptibility of human c-Ha-ras proto-oncogene transgenic rats to carcinogenesis: a cancer-prone animal model. Cancer Sci. 96, 309–316.

Wu, J., Liu, W., Xue, C., Zhou, S., Lan, F., Bi, L., Xu, H., Yang, X., Zeng, F.D., 2009. Toxicity and penetration of TiO_2 nanoparticles in hairless mice and porcine skin after subchronic dermal exposure. Toxicol. Lett. 191, 1–8.

Xu, J., Futakuchi, M., Iigo, M., Fukamachi, K., Alexander, D.B., Shimizu, H., Sakai, Y., Tamano, S., Furukawa, F., Uchino, T., Tokunaga, H., Nishimura, T., Hirose, A., Kanno, J., Tsuda, H., 2010. Involvement of macrophage inflammatory protein 1alpha (MIP1alpha) in promotion of rat lung and mammary carcinogenic activity of nanoscale titanium dioxide particles administered by intra-pulmonary spraying. Carcinogenesis 31, 927–935.

Yamanaka, K., Ohtsubo, K., Hasegawa, A., Hayashi, H., Ohji, H., Kanisawa, M., Okada, S., 1996. Exposure to dimethylarsinic acid, a main metabolite of inorganic arsenics, strongly promotes tumorigenesis initiated by 4-nitroquinoline 1-oxide in the lungs of mice. Carcinogenesis 17, 767–770.

Deficiency of the *Erc/mesothelin* gene ameliorates renal carcinogenesis in *Tsc2* knockout mice

Danqing Zhang,[1] Toshiyuki Kobayashi,[1] Tetsuo Kojima,[2] Kenji Kanenishi,[3] Yoshiaki Hagiwara,[1,4] Masaaki Abe,[1] Hidehiro Okura,[1] Yoshitomo Hamano,[1] Guodong Sun,[1] Masahiro Maeda,[4] Kou-ichi Jishage,[5] Tetsuo Noda[6] and Okio Hino[1,7]

[1]Department of Pathology and Oncology, Juntendo University School of Medicine, Tokyo; [2]Chugai Pharmaceutical Co. Ltd, Shizuoka; [3]Department of Perinatology and Gynecology, Kagawa University School of Medicine, Kagawa; [4]Immuno-Biological Laboratories Co. Ltd, Gunma; [5]Chugai Research Institute for Medical Science, Inc., Shizuoka; [6]The JFCR-Cancer Institute, Tokyo, Japan

(Received June 22, 2010/Revised October 14, 2010; December 20, 2010/Accepted December 22, 2010/Accepted manuscript online January 4, 2011)

Genetic crossing experiments were performed between tuberous sclerosis-2 (*Tsc2*) KO and expressed in renal carcinoma (*Erc*) KO mice to analyze the function of the *Erc/mesothelin* gene in renal carcinogenesis. We found the number and size of renal tumors were significantly less in *Tsc2*+/−;*Erc*−/− mice than in *Tsc2*+/−;*Erc*+/+ and *Tsc2*+/−;*Erc*+/− mice. Tumors from *Tsc2*+/−;*Erc*−/− mice exhibited reduced cell proliferation and increased apoptosis, as determined by proliferating cell nuclear antigen (Ki67) and TUNEL analysis, respectively. Adhesion to collagen-coated plates *in vitro* was enhanced in *Erc*-restored cells and decreased in *Erc*-suppressed cells with siRNA. Tumor formation by *Tsc2*-deficient cells in nude mice was remarkably suppressed by stable knockdown of *Erc* with shRNA. Western blot analysis showed that the phosphorylation of focal adhesion kinase, Akt and signal transducer and activator of transcription protein 3 were weaker in *Erc*-deficient/suppressed cells compared with *Erc*-expressed cells. These results indicate that deficiency of the *Erc/mesothelin* gene ameliorates renal carcinogenesis in *Tsc2* KO mice and inhibits the phosphorylation of several kinases of cell adhesion mechanism. This suggests that Erc/mesothelin may have an important role in the promotion and/or maintenance of carcinogenesis by influencing cell-substrate adhesion via the integrin-related signal pathway. (*Cancer Sci*, doi: 10.1111/j.1349-7006.2011.01846.x, 2011)

Expressed in renal carcinoma (*Erc*) was identified as an inducible gene during renal carcinogenesis in the Eker (tuberous sclerosis-2 [*Tsc2*] mutant) rat. The background of this research originates from our studies of the mechanism of multistep carcinogenesis in an animal model involving the *Tsc2* mutant gene using the Eker rat.[1–4] Development of hereditary renal carcinomas in the Eker rat is initiated by a somatic second hit[5] of the *Tsc2* gene. To elucidate the "steps" involved in *Tsc2*-deficiency, genes induced during renal carcinogenesis were cloned in the Eker rat and *Erc* was identified as a novel gene. Subsequently, it was revealed that *Erc* is a homologue of the human *mesothelin* gene.[6] Also, Erc protein is a homologue of a 31-kDa megakaryocyte potentiating factor (MPF), which can stimulate the megakaryocyte colony-forming activity of murine interleukin-3 in mouse bone marrow cell culture. Moreover, Erc protein was also cloned as an antigenic mesothelin for the monoclonal antibody K1 raised against ovarian cancer.[7–9]

Erc/mesothelin protein is a glycosyl phosphatidylinositol (GPI)-anchored membrane glycoprotein that is expressed in normal mesothelial cells. It is also highly expressed in several species of malignant tumors, such as mesothelioma as well as ovarian and pancreatic cancers.[10–13] Its primary product, a 71-kDa precursor of protein, can be physiologically cleaved by a furin-like protease into two fragments. A 31-kDa amino-terminal fragment (MPF, described hereafter as N-Erc/mesothelin) is released into the extra-cellular fluids, while a 40-kDa carboxy-terminal fragment (C-Erc/mesothelin) remains in the cell membranes.[10–16] Soluble N-Erc/mesothelin in serum is already being utilized as a diagnostic tumor marker[14–16] and anti-C-Erc/mesothelin immunotoxin therapy has been reported to be effective for mesothelioma and some C-Erc/mesothelin-expressing cancers.[10] Several *in vitro* studies have suggested that activation of cancer-associated signaling pathways increases Erc/mesothelin expression, and Erc/mesothelin may play a role in tumor adhesion, dissemination, metastasis and resistance against cell death.[9,10,17–22] However, mutant mice in which both copies of the mesothelin gene were inactivated showed no detectable abnormalities when compared with wild-type littermates.[23] Thus, it is conceivable that Erc/mesothelin may have a specific role in carcinogenesis as well as pathogenesis.

The *Erc/mesothelin* gene, described hereafter as *Erc*, is also highly expressed in renal tumor cells from *Tsc2* KO heterozygous mutant (*Tsc2*+/−) mice, that develop hereditary renal tumors presenting as cysts, cyst-adenomas, and solid adenomas that histologically resemble those in the Eker rat.[24]

In this study, *Tsc2*+/−;*Erc*−/− double mutant mice were generated through meiotic recombination and several renal tumor cell lines were established. The phenotypes of the *Tsc2* KO mice with or without *Erc* expression were compared and functions of the *Erc* gene in carcinogenesis were analyzed *in vivo* and *in vitro*. We report here that the development of renal tumors was significantly reduced in *Tsc2*+/−;*Erc*−/− mice, as compared to *Tsc2*+/− (*Erc* WT) or *Tsc2*+/−;*Erc*+/− mice and the several phosphorylation events mediated by integrin and the mammalian target of rapamycin (mTOR) were disrupted in *Tsc2*;*Erc* double deficient renal tumor cells.

Materials and Methods

Gene targeting and generation of *Erc* knockout mouse and crossing with *Tsc2* knockout mouse. Genomic DNA clones covering *Erc* were prepared from a mouse genomic DNA library and used for construction (see Data S1 and Fig. S1 for details).

Tumor measurement and tissue preparation. Mice were sacrificed at 18 months of age. The visible tumors on the renal surface were counted and measured with a caliper for length and width. The size of a tumor was defined to be the tumor's mean diameter: (length [mm] + width [mm])/2. Mice were divided into three groups according to the size of their largest tumor: small (<3 mm), large (3–10 mm) and extra-large (>10 mm). Tissues were fixed in 10% neutral formalin and paraffin sections (3 μm each) were prepared for examination.

[7]To whom correspondence should be addressed. E-mail: ohino@juntendo.ac.jp

doi: 10.1111/j.1349-7006.2011.01846.x

Cell adhesion assay. The assay was performed according to a method described previously[25] with minor modifications and with type I collagen-coated 24-well plates (Iwaki, Tokyo, Japan). Briefly, after blocking nonspecific adhesion with 1% bovine serum albumin in PBS, 1×10^5 cells suspended in 1.0 mL of 10% FCS/RPMI-1640 were added to each well and the cells were allowed to adhere for 1 h at 37°C in a 5% CO_2 incubator. After washing with PBS, the remaining cells were stained with 0.5% crystal violet in 20% methanol for 30 min and then washed away with water. The stained cells were solubilized in 20% acetic acid and the absorbance of the solution was read in a microplate spectrophotometer (Benchmark Plus; Bio-Rad, CA, USA) at 595 nm. Three independent experiments were performed in quadruplicate.

Transplantation assay. BALB/c nude mice were injected subcutaneously with 5×10^6 tumor cells in 100 μL of serum-free medium. After tumors appeared, the tumors were measured weekly with a caliper for length, width and height and the volume was calculated using the following formula: tumor volume (mm^3) = length (mm) × width (mm) × height (mm)/2.

Statistical analysis. All discrete values, expressed as mean ± SEM, were analyzed using Student's *t*-test. *P*-values of <0.05 were considered statistically significant.

See Supporting Information (Data S1) for additional methods.

Results

Establishment of *Tsc2;Erc* double knockout mice. *Trans*-compound double heterozygous mutant (*Tsc2*+/− and *Erc*+/−) male mice were mated with C57BL/6J (WT) females (Fig. 1a). Of the 109 offspring, there was a single mouse carrying both *Tsc2* and *Erc* mutations that is a *cis*-compound double heterozygous mutant (Fig. 1b, white star), provisionally designated Erc109.

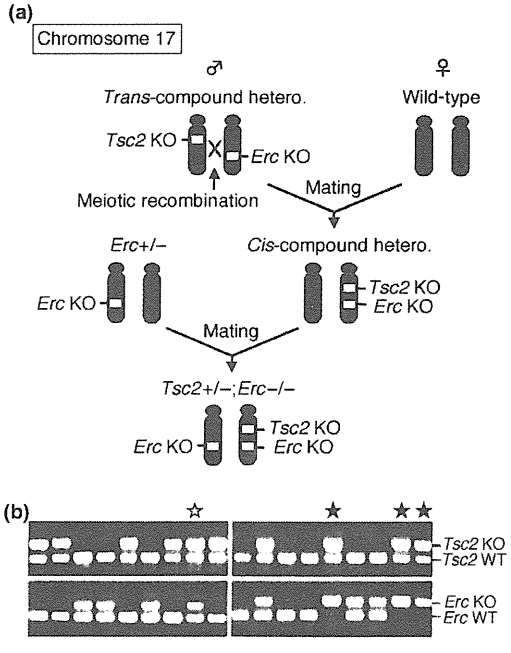

Fig. 1. Generation of tuberous sclerosis-2 (*Tsc2*); expressed in renal carcinoma (*Erc*) double KO mouse. (a) Outline of intercrosses. Only *Erc*-deficient mouse is denoted after second mating. (b) Genotyping of genomic DNA by PCR. Representative results of offspring from first cross (left panels) and second cross (right panels) are shown. Upper and lower panels show genotypes of *Tsc2* and *Erc*, white and black stars indicate the *Tsc2*+/−;*Erc*+/− (*cis*-compound heterozygous) mutant and the *Tsc2*+/−;*Erc*−/− mutant, respectively.

Tsc2+/−;*Erc*−/− mice (Fig. 1b, black stars) were established by mating Erc109 (*Tsc2*+/−;*Erc*+/−) with *Erc* KO mice (Fig. 1a). Absence of Erc protein in *Tsc2*+/−;*Erc*−/− mice was confirmed immunohistochemical staining of the lung mesothelium (Fig. 2a) using anti-mouse C-Erc/mesothelin rabbit polyclonal antibody (Fig. S2).

Reduced renal tumor development in *Tsc2*+/−;*Erc*−/− mice. Renal tumor development was examined in *Tsc2*+/− (*Erc* WT), *Tsc2*+/−;*Erc*+/− and *Tsc2*+/−;*Erc*−/− mice (Fig. 2b–f). Renal tumors were developed in all of the above mice at 18 months of age (Fig. 2b,c,f). However the number (Fig. 2d) and size (mean diameter; Fig. 2b,e,f) of visible tumors on the renal surface were significantly reduced in the *Tsc2*+/−;*Erc*−/− mice. In *Tsc2*+/− as well as *Tsc2*+/−;*Erc*+/− mice, frequent development of tumors of large-size (≥3 mm) were observed in both females and males. There were 59.3% (16 of 27) female and 58.3% (14 of 24) male *Tsc2*+/− mice and 58.6% (17 of 29) female and 57.1% (16 of 28) male *Tsc2*+/−;*Erc*+/− mice that developed large-size tumors. In contrast, only two of 20 females (10.0%) and one of 15 males (6.7%) of *Tsc2*+/−;*Erc*−/− mice showed such large-size tumors (Fig. 2f), although they commonly exhibited carcinogenesis. Moreover, extra-large-size (>10 mm) tumors were seen in *Tsc2*+/− and *Tsc2*+/−;*Erc*+/− mice (11 and 13 cases, respectively) but were not found in *Tsc2*+/−;*Erc*−/− mice (Fig. 2b,f). These observations suggest that the progression of renal tumors in *Tsc2* mutant mice was suppressed by *Erc*-deficiency.

Decreased proliferation in renal tumors from *Tsc2*+/−;*Erc*−/− mice. To elucidate the cellular basis for the effects of *Erc*-deficient on proliferation and apoptosis of renal tumors, the paraffin-embedded renal tumor sections were stained with anti-mouse Ki67 (a proliferating cell nuclear antigen) by immunohistochemistry and TUNEL analysis, respectively (Fig. 3). Tumors derived from *Tsc2*+/−;*Erc*−/− mice not only were significantly reduced tumor cell proliferation (Fig. 3a) but also showed increased apoptosis (Fig. 3b) compared with tumors from *Tsc2*+/−;*Erc*−/− mice although *Erc*-deficient tumors exhibited a mild increase in apoptosis status (Fig. 3c).

Positive effects of Erc on collagen-mediated cell-substrate adhesion in renal tumor cell lines. To conduct an *in vitro* functional analysis of Erc, renal tumor cell lines were established from *Tsc2*+/−;*Erc*−/− mice. Then, *Erc* expression was restored in one of the established cell lines (DE42L-T1-9) by stable transduction of an *Erc* expression vector and the expression of Erc protein was shown by Western blot (Fig. 4a). *Erc*-restored cells (T1-9Ep10 and T1-9Ep13) were found to be more competent to adhere on the collagen-coated plates than *Erc*-deficient (parental and empty-vector) cells (Fig. 4b). To ascertain that the increased adhesion was due to the function of Erc, the expression of Erc in *Erc*-restored cells was re-suppressed by RNAi and the effect of Erc-suppression was verified by RT-PCR and Western blot (Fig. 4c). The adhesion of these cells on collagen-coated plates was significantly reduced by the suppression of *Erc* (Fig. 4d), confirming that Erc positively regulates cell-substrate adhesion.

Suppression of tumorigenesis with *Erc*-suppression in *Tsc2*-deficient renal tumor cells. *Erc*-suppressed cells were established by stable expression of shRNA from the MKOC1-277 cell line that is a *Tsc2*-deficient mouse renal tumor cell line with highly expressed *Erc* (Fig. 5a). When *in vivo* tumorigenicity was examined by subcutaneous injections of cells into nude mice, tumors generated from the *Erc*-suppressed cells were smaller and paler than those from the control shRNA cells that showed robust tumorigenesis (Fig. 5b,c). Conversely, when *Erc*-restored cells were assayed, they exhibited more vigorous growth compared with *Erc*-deficient (empty-vector) cells (Fig. S3). These data suggest that Erc exerts a positive effect on tumorigenicity.

doi: 10.1111/j.1349-7006.2011.01846.x

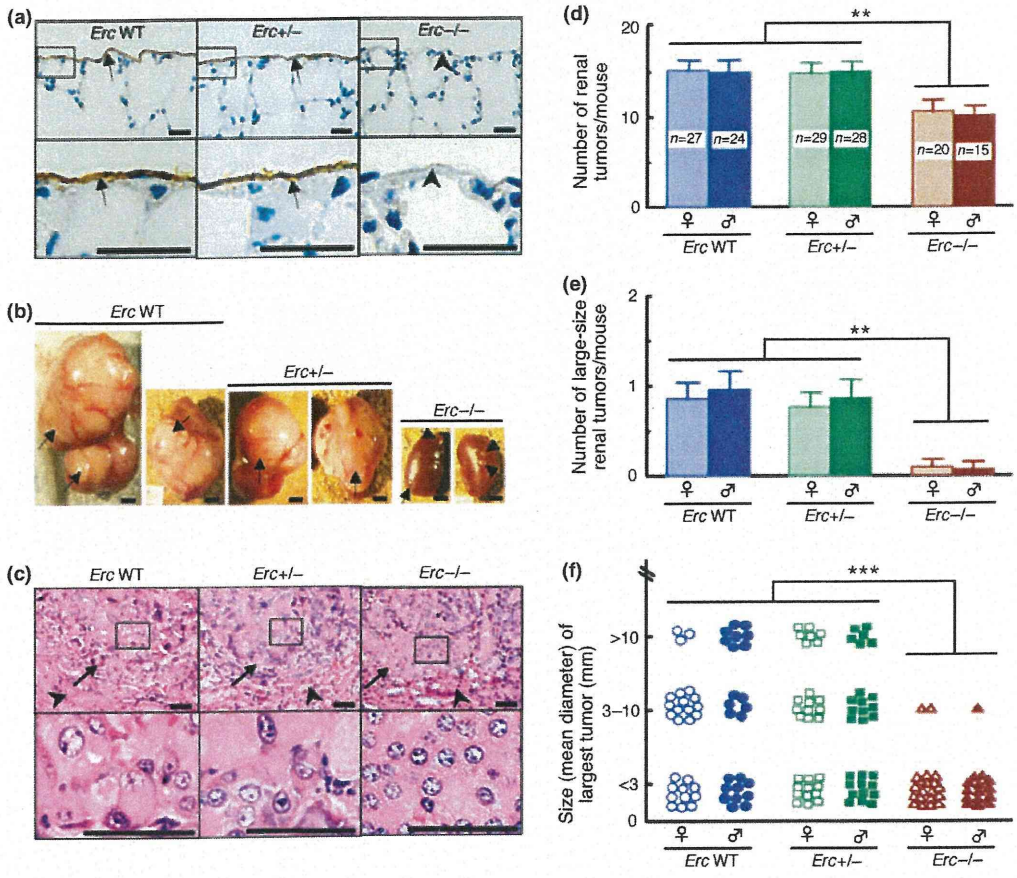

Fig. 2. Reduction of the number and size of renal tumors in expressed in renal carcinoma (*Erc*)-deficient mice. (a) Immunohistochemical staining of anti C-Erc/mesothelin show the positive reactions (arrows) in lung mesothelium of tuberous sclerosis-2 (*Tsc2*)+/– (*Erc* WT) and *Tsc2*+/–;*Erc*+/– mice, but not in *Tsc2*+/–;*Erc*–/– mice (arrowheads). Scale bars = 20 μm. (b) Representative macroscopic findings of the renal tumors (arrows) in 18-month-old mice. Scale bars = 3 mm. (c) H&E staining of sections of renal tumors of above mice. Arrows and arrowheads indicate tumors and normal tissues, respectively. Scale bars = 40 μm. (d) The number of renal tumors was evaluated and expressed as average number per mouse. Values are means ± SEM; $^{**}P < 0.01$. Number of mice measured in each group is shown in columns. (e) The number of large-size (≥3 mm) tumors was selected from (d) and expressed as average number per mouse. Values are means ± SEM; $^{**}P < 0.01$. The number of mice measured in each group is the same as (d). (f) The mice were categorized into three groups according to the size (mean diameter) of the largest tumor that the mouse harbored. Points = the largest tumor of each mouse; $^{***}P < 0.001$. The number of mice measured in each group is the same as (d). The large-size and extra-large-size tumor numbers in the *Erc*–/– mice are significantly less when compared with the other mouse strains.

Modulation of integrin-related signaling by Erc expression. Integrin β1 is a major subunit of collagen receptors[26] and is required for collagen-mediated proliferation of cancer cells.[27–29] Signals from the integrin complex are transmitted through the phosphorylation of focal adhesion kinase (FAK).[30–32] To determine if Erc expression affects cell adhesion through integrin-related signaling, the expression of integrin β1 and the phosphorylated status of downstream molecules were compared among the indicated cell lines (Fig. 6). As previously reported, two major bands were observed in Western blots of integrin β1,[33–37] namely a partially glycosylated 115 kDa precursor and a fully glycosylated 135 kDa mature form. These bands were disappeared or abolished and a band of core peptide (86 kDa) was appeared upon mild (2 μg/mL) tunicamycin (a *N*-glycosylation inhibitor) treatment, confirming the characteristics of integrin β1 (Fig. S4). Mature integrin β1 was dominant in *Erc*-deficient (parental and empty-vector) cells, while the expression of integrin β1 shifted to the precursor in *Erc*-restored cells (Fig. 6a). Reciprocally, levels of the precursor integrin β1 were decreased in *Erc*-suppressed cells compared with *Erc*-expressed (parental and control shRNA) cells (Fig. 6b). Although direct evidence has not yet been obtained, it is plausible that the expression of mature integrin β1 may be regulated by feedback from cell adhesion machinery regulated by Erc.

The level of phosphorylation of FAK (Tyr925) correlated with Erc expression in cells tested (Fig. 6a), suggesting that the signals downstream of integrin are upregulated by Erc. Further tests were conducted for the phosphorylation of Akt (Ser473), S6K (Thr389) and rpS6 (Ser235/236) with three *Tsc2*-related molecules implicated in insulin signaling and mTOR pathway.[38,39] In *Erc*-restored cells, phosphorylation of Akt (Ser473) and rpS6 (Ser235/236) were found to be more robust while phosphorylation of S6K (Thr389) also was induced although to a lesser extent (Fig. 6a). In other words, the phosphorylation of rpS6 (Ser235/236), catalyzed by S6K as is generally known, was shown to be remarkably weaker than S6K (Thr389) in *Erc*-deficient cells and induced in *Erc*-restored cells. The level of phosphorylation of signal transducer and activator of transcription protein 3 (Stat3; Tyr705) is constitutively higher in *Erc*-restored cells than in *Erc*-deficient cells. Positive effects of Erc on these phosphorylated events were also verified in *Erc*-suppressed cells compared with *Erc*-expressing cells (Fig. 6b).

To investigate the molecular basis for the increase in cell adhesion in the *Erc*-restored cells, the cells were treated with